A MODEL FOR ABRASIVE POLYMER WEAR

by

John Henry Herold II

Dissertation submitted to the Graduate Faculty of the

Virginia Polytechnic Institute and State University

in partial fulfillment of the requirements for the degree of

DOCTOR OF PHILOSOPHY

in

Mechanical Engineering

APPROVED:

Dr. N. S. Eiss, Jr., Chairman

Dr. J. B. Jones, Dept. Head

Dr. L. D. Mitchell

Dr. H. H. Mabie

Dr. E. G. Henneke

June, 1980

Blacksburg, Virginia

ACKNOWLEDGMENTS

The author is indebted to Dr. Norman S. Eiss, Jr., Chairman of his committee, employer, colleague, and friend. His patience, tolerance, guidance, and availability far exceeded all reasonable expectations. The author considers himself truly fortunate for having had the opportunity to work with this man. The author also expresses his appreciation to the other members of his committee for their time and patient tutelage.

The author thanks his parents and friends for their support and encouragement throughout his educational program.

The author is at a lack to adequately express his appreciation to his wife, Pam. She, through her moral and financial support, and through her ceaseless quiet sacrifice of service, made these last years of study both possible and pleasant. David Herold, yet another gift to the author from his wife, is also thanked for the inspiration, growth, and joy the author has derived from him.

TABLE OF CONTENTS

LIST OF FIGURES

LIST OF FIGURES (cont'd)

LIST OF FIGURES (cont'd)

LIST OF TABLES

NOMENCLATURE

A_a	apparent area of contact
A_r	real area of contact
Ar_i	area of contact associated with asperity i
BAR	Bearing Area Ratio
c , C^*	yield stress multiplier, p_m/Y
C	constant used in Blok-Halliday criterion
d	sliding distance
D , D	diameter of wear face of polymer pin
D_s , D_S	slider length
dl , DL	incremental sliding distance
dV	incremental volume
E	Young's modulus
G , G	particle formation rate factor
H	hardness
i	index referring to a given asperity
I	plasticity index
k	wear coefficient, probability per unit encounter of a wear particle being produced
L , L	length of sampled profile
p , P	penetration depth
p_m	flow pressure
pm_i	pressure at asperity i

* Characters appearing after a comma indicate font used in figures.

r , R	radius used in Rabinowicz's wear equation
R , R	radius of wear track on ground steel disks
R_a	Arithmetic average roughness
S	polymer breaking strength in tension
T_g	glass transition temperature
T_m	crystalline melting point
V	wear volume
V_{m_i}	void volume at wear site i, $D \cdot VA_i$
V_{u_i}	wear volume at wear site i for an unfilled void volume
VA_i	void area at wear site i
W	normal load
WA_i	wedge area at wear site i
WH_i	wedge height at wear site i
W_i	normal load supported by asperity i
WL_i	wedge length at wear site i
W_t	total normal load
x , X	penetration depth used in Rabinowicz's wear equation
Y	yield strength

Greek Symbols

β	average radius of curvature of peaks
β , B	wedge angle
β_c	critical or transition angle between the rigid-plastic and elastic-plastic mode of deformation
γ , γ	slope of profile as a function of position
ε	elongation at break
θ	angle of cone used in Rabinowicz's model
ν	Poisson's ratio
σ	standard deviation of the asperity heights
ϕ , ϕ	polymer shear angle

1. INTRODUCTION

Polymers are being utilized in an ever-increasing range of design applications. While they do not excel in any one material property, certain polymers do possess a combination of properties, e.g., strength, wear resistance, lightness, and formability, often desired of machinery components. These engineering polymers are classified as linear high polymers, their outstanding characteristic being their high molecular weight and the chainlike linkage of repeat units [1]*. Table 1 lists a representative group of engineering polymers along with their name abbreviation, repeat units, glass transition temperature (T_g), and crystalline melting point (T_m).

In design applications, a material is often chosen for a specific property, providing its other properties do not preclude its use. Glass is often chosen for its transparency and steels for their strength. Polymers, in turn, are often chosen for their friction and wear characteristics. Just as design with steel has required an accurate characterization of the strength properties of steel, design with polymers has required the ability to characterize and predict friction and wear properties of polymers.

The performance of polymers in dry sliding contact has proven difficult to predict. The wear resistance of the polymer is determined not only by its material properties, but also by external conditions such as operating load and speed, and the topography and material

* Numbers in brackets refer to similarly numbered references listed in Reference section.

Table 1. Various Linear High Polymers With Name Abbreviations, Repeat Units, Glass Transition Temperature (T_g), and Crystalline Melting Point (T_m) [2].

Polymer (Name Abbreviation)	Repeat Unit	T_g(°C)	T_m(°C)
Polyhexamethylene adipamide (Nylon 6-6)	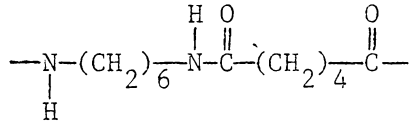	50	265
Polypropylene (PP)	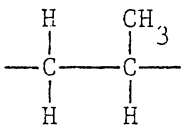	-10, -18	176
Polyethylene (PE)	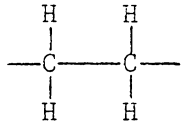	-120	137
Polytetrafluoroethylene (PTFE)	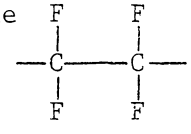	-50, 126	327
Polychlorotrifluoro-ethylene (PCTFE)	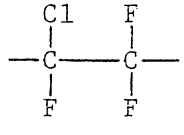	45	220
Polyvinylchloride (PVC)	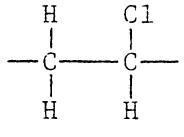	87	212
Polystyrene (PS)	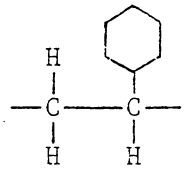	100, 105	240

Table 1. Various Linear High Polymers With Name Abbreviations, Repeat Units, Glass Transition Temperature (T_g), and Crystalline Melting Point (T_m) [2].

(Continued)

Polymer (Name Abbreviation)	Repeat Unit	T_g(°C)	T_m(°C)
Polyhexamethylene sebacamide (Nylon 6-10)	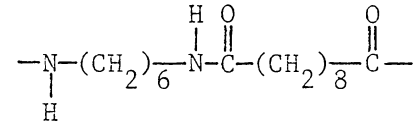	40	227
Polymethylmethacrylate (PMMA)	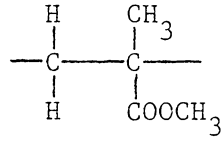	105	160
Polyisobutylene	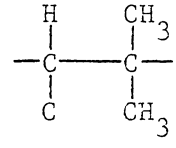	-70, -60	128
Polyoxymethylene (POM)	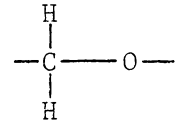	-50, -80	181
Polycaprolactam (Nylon 6)	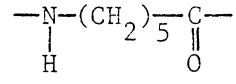	50	225
Polyisoprene	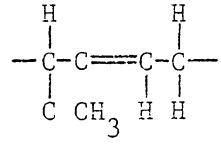	-73	28

properties of the counterface. In the initial stages of the wear of a polymer against a harder counterface, polymer transfers to the counterface. If the counterface is smooth, some polymers such as PTFE and HDPE (high density PE) transfer as continuous thin films via the adhesion mechanism [3]. If the counterface is rough, most polymers will transfer in discrete lumps via the abrasion mechanism [4-6]. As sliding continues, other mechanisms such as fatigue may dominate the transfer process [5-7]. In some cases the wear rate of the polymer may be controlled by the rate at which loose wear particles can be expelled from the system, creating a strong dependence of wear rate on the degree of containment the system imposes on the debris [8]. In addition to transfer to the counterface, some polymers wear by roll formation [6]. The initial transfer process is often followed by back transfer in which two or more wear mechanisms can be equally important.

Depending on the particular wear system configuration, abrasive wear of polymers can often be divided into two regimes: 1) the initial regime of wear, often referred to as "break-in", involving the filling of voids in the counterface, and 2) the steady state regime of wear, where the wear rate is equal to the rate of wear debris removal from the wear system. This dissertation documents the development of a predictive model for polymer wear during the initial stage of abrasive polymer wear. This model does not attempt to correlate wear with one or more statistical parameters of the counterface as is often done; but instead simulates wear on an event-by-event basis. The primary input to the model is a digitized profile of the metal counterface.

Once developed, this model is then used to generate wear predictions for comparison with the results of experimental wear tests of previous researchers. Finally, a discussion of the limitations of this model is presented along with recommendations for possible refinements and expansion of the model to encompass, for example, the steady state transport wear regime.

2. LITERATURE REVIEW

The polymer wear which occurs in polymer/steel sliding systems, like the wear in metal/metal sliding systems, is typically classified by mechanism into four types [2]. These types are: 1) adhesive or sliding wear, 2) thermal and oxidative wear, 3) surface fatigue, corrosion and cavitation, and 4) abrasive wear. In any one system, all of these types of wear are usually present; however, one type is usually predominant. This dissertation is limited to the study of the abrasive mechanism of wear which dominates in the early stage (the break-in period) of polymer/steel sliding systems. The vast majority of polymer wear literature, however, attends only to the steady state regime of polymer wear, owing to interest in the use of polymers as unlubricated bearings.

The polymer wear research of Archard and Hirst [9] provides a good starting point in polymer wear literature. Although their data were based on long running, multiple pass experiments, their observations and the resultant wear law are important. Subsequent researchers, in proposing abrasive wear models, have sought to validate these models by showing them to yield the relationship observed by Archard and Hirst. This is ironic since the abrasive wear mechanism usually dominates only in the early stage of polymer wear, and this regime is specifically neglected by Archard and Hirst as a transient startup phenomenon.

Archard and Hirst reported in 1956 on wear experiments with polymer sliding on metal surfaces, PMMA, PTFE, PE, and several thermosets were tested on a pin-ring type machine. By varying the apparent area of contact, A_a, and the normal load, W, they found

the wear volume, V, could be expressed as

$$V = kdW/p_m \qquad (1)$$

where d is the sliding distance, p_m is the polymer flow pressure, and k is a constant called the wear coefficient. The constant k was interpreted as the probability per unit encounter of a wear particle being produced. The real area of contact, A_r, equals W/p_m [10], where p_m is a material constant usually taken to be equal to three times the yield strength of the softer material. This relation between flow pressure and yield strength will be further discussed in section 3.2. Values of k computed for their data were 7×10^{-6} for PMMA, 2.5×10^{-5} for PTFE, 1.3×10^{-7} for PE, and from 0.3 to 7.5×10^{-6} for the thermosets tested. Once again it should be noted that these were long running, multiple pass experiments where a constant wear rate was achieved.

In 1965 Rabinowicz [11, p. 168] derived an expression for abrasive wear in which a hard conical indenter penetrates a softer material, and is then traversed as shown in Fig. 1. A single conical asperity supporting a load W will penetrate the softer material such that

$$W = p_m \cdot A_r = p_m \cdot \pi r^2 \qquad (2)$$

where p_m is again the flow pressure of the softer material. The projected area of the penetrating portion of the cone in the vertical plane is rx. Hence, when the cone is traversed an elemental distance dl, it will sweep out an elemental volume dV equal to

$$dV = r \cdot x \cdot dl = r^2 \tan\theta \cdot dl = \frac{W \cdot \tan\theta \cdot dl}{\pi p_m} \qquad (3)$$

or,

$$\frac{dV}{dl} = \frac{W \cdot \tan\theta}{\pi p_m} \; . \qquad (4)$$

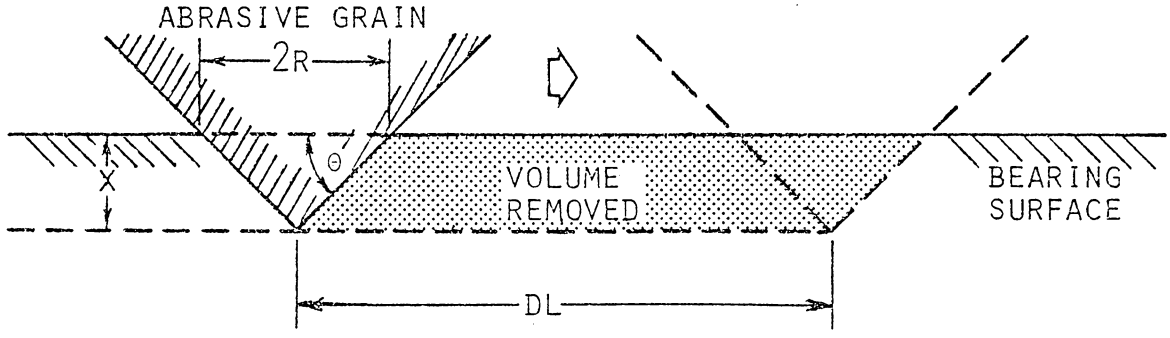

Figure 1. Abrasive Wear Model in which a cone removes material from a surface, from Rabinowicz [11, p. 168].

Combining the contributions of several asperities

$$\frac{dV}{dl} = \frac{W_t \cdot \overline{\tan\Theta}}{\pi p_m} \tag{5}$$

where $\overline{\tan\Theta}$ is the weighted average of the $\tan\Theta$ values of all the individual cones, and W_t is the total normal load.

Lancaster [5] states that Eq. 5, when integrated, leads to

$$V = \frac{kWd \cdot \overline{\tan\Theta}}{p_m} \tag{6}$$

where d is the total distance slid, and k is a constant interpreted to express the face that not all the material involved in the deformation is removed from the system as debris, but that some is simply displaced plastically. Lancaster [4] shows that the volume of wear is proportional to $\overline{\tan\Theta}$ for soft metals but not for polymers. For tin the expected relationship is true for all angles of the cone, but only holds for polymers when the base angle, Θ, is very large. Lancaster concludes that during sliding against roughnesses commonly encountered in engineering practice, the deformation of polymers is partly elastic and partly plastic, and relative proportion will vary with the roughness.

Two criteria are available to determine the point in the roughness scale at which plastic deformation begins. Although they were developed for applications involving a rough deformable surface being pressed against a hard plane, it is assumed they are equally applicable to the inverse case of a hard asperity penetrating a softer

solid material. The Blok-Halliday criterion [12] states that the limiting slope of an asperity which can just be flattened by a rigid plane into the general plane of a surface is

$$\tan\Theta_{lim} = C \frac{H}{E} (1-\nu^2) \qquad (7)$$

where H is the hardness of the material, E is Young's modulus, and ν is Poisson's ratio for the deforming material, in this case the polymer. For the onset of plastic flow, C=0.8; and for full plasticity, C=2.0. The second criterion is the "plasticity index", which was introduced by Greenwood and Williamson [13], and is given as

$$\bar{I} = \frac{E}{H} \left[\frac{\sigma}{\beta}\right]^{1/2} \qquad (8)$$

where σ is the standard deviation of the asperity heights, and β is their average radius of curvature. The elastic/plastic transition is considered to occur in the neighborhood of I=1. Lancaster interprets his data and the aforementioned indices to indicate that a ground surface with an arithmetic average roughness, R_a, on the order of 25.4 μm or more is required for significant plastic deformation of the polymer. Ground surfaces commonly have a R_a roughness on the order of 0.05 - 3.0 μm. Therefore, based on Lancaster's analysis, a polymer sliding on ground surfaces can be expected to exhibit a considerable proportion of elastic deformation.

Orthogonal cutting theory (abbreviated OCT) [14,15,16,17] is of interest as a wear theory. The steel surfaces which are modeled in this study and which are used in supporting experimental work were produced

by a grinding process. As such they are taken to be a series of two-dimensional, parallel ridges and valleys which can be characterized by a single profile. As a polymer slider is traversed normal to the grinding lay, a given steel ridge can be envisioned to cut the polymer as a tool face might during a machining operation. Hence, when a polymer is slid against a ground steel counterface, OCT might be used to determine forces and other parameters of the abrasive wear process. When used to predict wear rates it is identical to Rabinowicz's cone penetrator model except that in OCT the removal is assumed to occur along a cutter face of infinite width. Like Rabinowicz's cone model, OCT is based on the assumption that all the material in front of the tool is removed. Like Rabinowicz's cone model it grossly overpredicts wear both because it does not allow for elastic and plastic polymer flow around the asperity, and because it does not allow for the eventual, indeed in some cases rapid, filling of the valleys in the steel surface with wear debris. This filling is analogous to the filling of a file when used on soft metals.

A file serves as an excellent demonstration of the two-dimensionality and the restricted valley region of ground surfaces. In OCT, the chip removed is assumed to travel along the tool face, away from the cutting region, in an unrestricted manner. But in the case of a file or a ground surface, the chip is restrained to the valley region by the next ridge. Thus the amount that can be removed by a given ridge is limited to the available valley volume.

While OCT cannot be used alone as a wear predictor, it does provide considerable insight into the fracture mechanics of wear. OCT predicts a plane of maximum shear stress which, in turn, can be used to help predict the shape of wear fragments. This feature of OCT will be further discussed in section 3.3.

3. DEVELOPMENT OF WEAR MODEL

3.1. Philosophy

The development of this abrasive wear model follows a simple sequence. First, the process of pressing the polymer (assumed smooth) against the rough metal counterface is modeled, providing the relative positions of the polymer and metal prior to sliding. This relative positioning is determined as a penetration depth of the polymer into the irregular surface of the metal.

The second section discusses the shape, form, and geometry of wear particles formed and retained by the metal surface during relative sliding. Although the geometry of these wear particles is discussed in terms of theoretical geometries, support for the geometries used in the model lies primarily in observations of wear debris.

The third section concludes the fundamental model development with a discussion of the rate of wear particle formation and its observed dependence on the elongation at break of the polymer. This variable rate, referred to as the wear particle formation rate, will be the crucial input allowing a variable proportion of the polymer encountering an asperity to be plastically and elastically deformed around the asperity without being removed as wear debris.

Lastly, the implementation of the model is discussed. This section presents a discussion of the interactive computer environment utilized and the methodology of computer based profilometry and data storage. It is this profile data which constitutes the primary input to the Fortran language description of the wear model.

3.2. Penetration Depth

Before sliding and subsequent abrasive wear can be modeled, the position of the polymer surface relative to the steel surface must be determined. A measure of the relative position is the penetration depth as shown in Fig. 2. The penetration depth is a function of the normal load, the polymer yield strength, the apparent area of contact, and the surface topography.

When a normal load, W_t, is applied to the polymer, the asperities of the metal surface penetrate the polymer until sufficient area develops to support the applied load. It is assumed that for asperity i, the area of contact, Ar_i, can be calculated by $Ar_i = W_i/pm_i$, where W_i is the normal load carried by asperity i, and pm_i is the pressure at asperity i. If the pressure is the same for each asperity, then $pm_i = p_m$, and the total real area of contact can be given as $A_r = W_t/p_m$. The flow pressure, p_m is often taken as constant and equal to 3Y where Y is the yield strength of the polymer in tension [10], which gives $A_r = W_t/3Y$. The real area of contact is usually less than the apparent area of contact, A_a, which defines the geometric limits of A_r. The ratio A_r/A_a is called the bearing area ratio, BAR, which is given by

$$BAR = \frac{A_r}{A_a} = \frac{W_t}{3YA_a} \qquad (9)$$

Thus BAR is a function of the normal load, the polymer yield strength, and the apparent area of contact.

If the polymer surface is assumed to be an ideally flat plane, for a given normal load, the asperities of the rough surface will penetrate to a depth at which the A_r is sufficient to support the load.

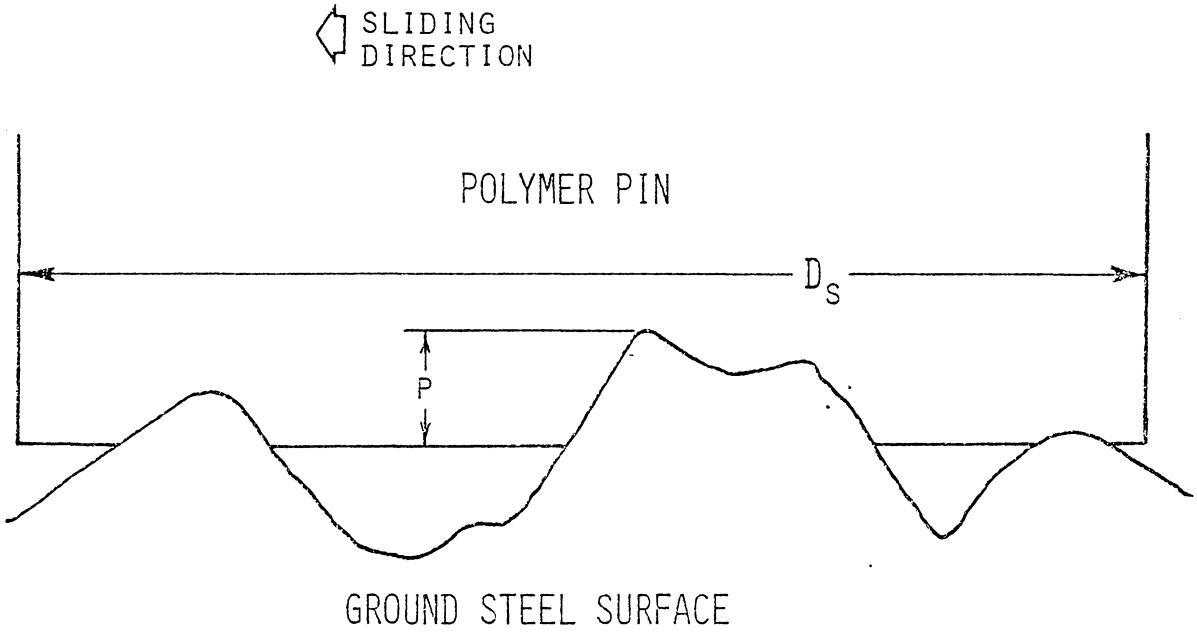

Figure 2. Illustration of penetration depth, p, and slider length, D_s.

The relationship between the real area of contact and the penetration depth is a statistical height parameter of the rough surface which is called the bearing area curve and is defined in Fig. 3. Therefore, given a BAR value and the bearing area curve for the metal surface, the penetration depth, p, of the highest metal asperity can be determined. Figure 3 shows three such curves for ground steel surfaces, each of a different roughness. In practice, the computer implementation of this wear model requires the BAR as input, and the penetration depth is subsequently determined prior to the modeling of the actual wear process.

In the abrasive wear model, the yield strength of the polymer in tension, Y, is known, and the flow pressure is required. A function of the form

$$p_m = cY \tag{10}$$

is used. In the current model a value of c = 3.0 is used.

In the field of indentation hardness testing, Y is calculated from a calculated p_m using Eq. 10. Hence, in this field there is interest in the validity of the assumption that for all materials and asperity (or indenter) geometries, c = 3.0 . The remainder of this discussion will be based on a better estimation of c obtained through the theory of indentation hardness.

If an asperity is modeled as a two-dimensional wedge [18] the deformation of the indented material (in this case the polymer) may be solved theoretically if it is assumed that the material is a perfectly rigid-plastic material [19]. Indeed for a perfectly rigid-plastic material indented by a rather blunt indenter, c = 3.0 [20]. Such a material is best described in terms of a simple tension experiment:

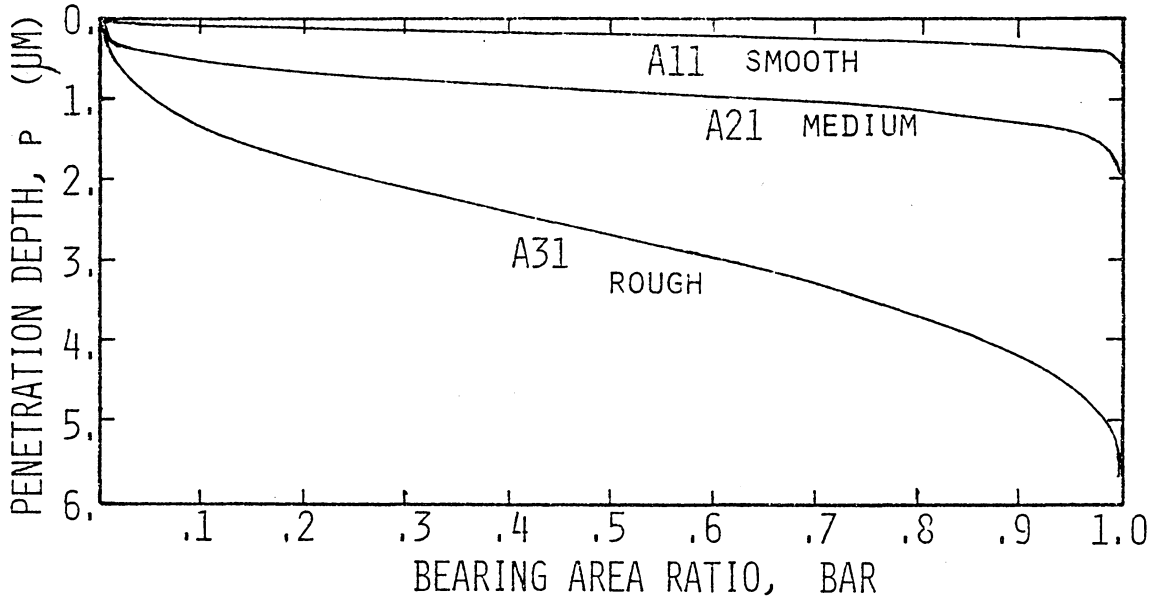

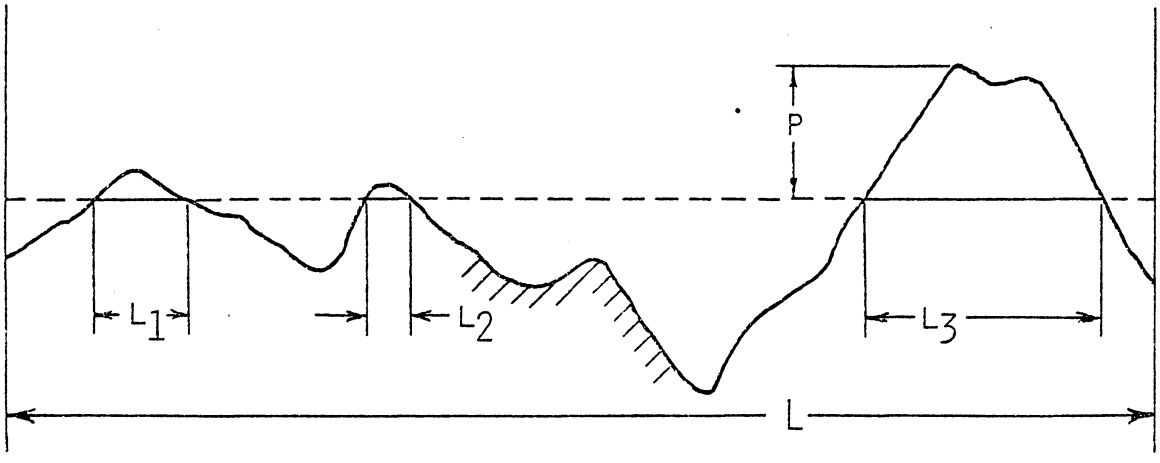

$$BAR(P) = \frac{1}{L}\sum_{I=1}^{3} L_I$$

Figure 3. Definition of and examples of BAR curves.

when subjected to tension it behaves perfectly rigidly, that is, the initial elastic deformation is zero, but at a critical stress it yields plastically with a constant yield stress (ideal-plasticity). Real materials, of course, are not ideally plastic, and some elastic deformation will occur. The value of c = 3.0 is based on the rigid confinement of the plastic material by the surrounding rigid material.

The situation changes for elasto-plastic materials. If the material is highly elastic, a different mode of deformation occurs [21]. Instead of the displaced material rising plastically around the indenter it is taken up in the bulk material by the elastic deformation, in a radial pattern, of the surrounding material, as shown in Fig. 4. Hence, two different deformation modes are observed. For ideal plastic flow, c = 3.0 . For elasto-plastic flow, c is given by the more complex relationship [22]

$$c = \frac{P_m}{Y} = \frac{1}{\sqrt{3}} \left[1 + \ell n \left(\frac{4}{3\pi} \frac{E}{Y} \tan\beta \right) \right] \qquad (11)$$

where β is the wedge angle as shown in Fig. 4, and where Poisson's ratio, ν, is assumed to have a value of 0.5 . As can be seen in the relationship expressed in Eq. 11, the value of c is a function of both the degree of elasticity, expressed as the ratio E/Y, and the angle of the indenter, β. Blunt indenters, whose angle β is small, tend toward low values of c. For values of (E/Y)tanβ less than about 2, the deformation is almost entirely elastic, and the mean pressure is given by the Hertzian equations. When (E/Y)tanβ reaches a value of 100, c has increased to about 2.8, and the material begins deforming in the rigid-plastic mode. In this mode, c assumes a constant value of 3.0 .

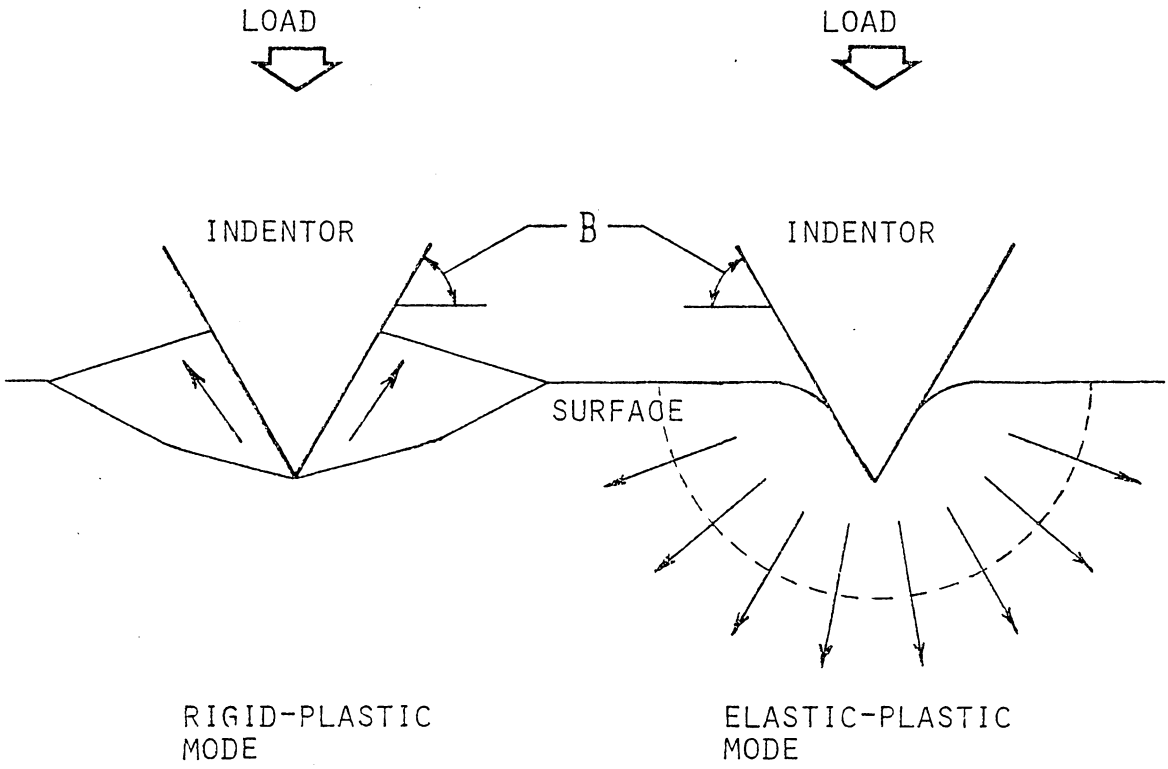

Figure 4. Illustration of rigid-plastic and elastic-plastic deformation modes.

Table 2 lists some bulk material properties for several materials [23] and includes the critical indenter angle, β_c. The angle β_c is defined as the smallest angle for which the rigid plastic deformation mode occurs. These values of β_c were determined by setting c = 3.0 in Eq. 11, and solving for β. As can be seen in Table 2, polymeric materials are more likely to deform in an elasto-plastic mode, since extremely large values of β are required for rigid-plastic deformation (as in Lancaster's [4] observations mentioned in the Literature Review section). Since PCTFE was one of the polymers used to acquire data in support of this model, Fig. 5 shows the variation of c with indenter angle for PCTFE. Hirst's value (from Table 2) for PCTFE of E/Y = 15.3 was used for this figure.

Given that one can determine a value for c and, therefore, a flow pressure p_m for polymers penetrated by wedges based on the aforementioned work, utilization of this p_m to predict a penetration depth in a wear model is still difficult. It is necessary to model any general asperity as a wedge-shaped indenter. In the modeling of an asperity as a wedge-shaped indenter, several questions arise such as:

a) Should it be required that the wedge-shaped indenter be equiangled?

b) Should the slope(s) of the wedge-shaped indenter be made equal to the slopes of the asperity at the points where the asperity intersects the plane of the polymer surface?

c) Should the height of the wedge-shaped indenter be set equal to the penetration of the asperity at its highest point?

Table 2. Bulk Properties of Various Engineering Materials [23].

material	E^{*} (GPa)	$Y^{\dagger}$ (MPa)	E/Y	$\beta_c^{\dagger\dagger}$ (deg)
lead alloy	16.08	19.42	828.	10.7
aluminum	68.94	150.05	459.	18.8
copper	124.06	390.32	318.	26.2
mild steel	207.61	775.73	268.	30.3
beryllium copper	110.33	1075.83	102.6	56.8
PTFE	0.60	26.28	22.6	81.8
PCTFE	1.17	76.10	15.3	84.4
Nylon	1.61	122.59	13.1	85.2
Perspex	2.47	221.64	11.2	85.9

* E, Young's modulus based on stress strain curves of compression test specimens.

† Y, yield stress in compression

†† $\beta_c = \tan^{-1}\left[\frac{156.52}{E/Y}\right]$

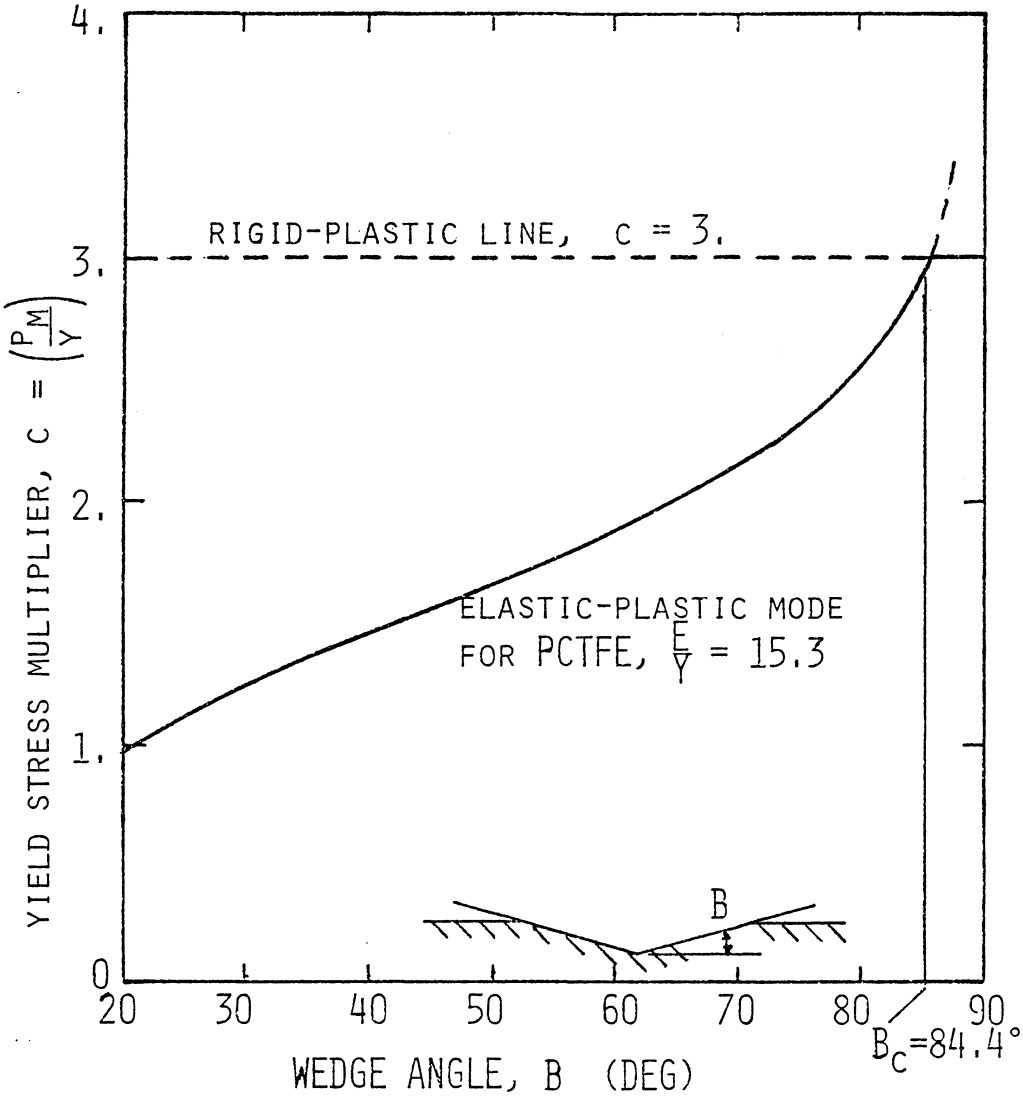

Figure 5. Variation of polymer flow pressure, p_m, with wedge angle, β, for PCTFE.

An entire study would be required to determine answers to these questions and is beyond the scope of this work. Therefore, a value of $c = 3.0$ was chosen for this work.

3.3. Geometry of Wear

In the previous section the penetration of asperities into the polymer was modeled. In this section, the geometry of the fracture of the bulk polymer and subsequent separation of a fragment of polymer from the bulk is modeled. The primary inputs to this stage of the wear model development are the observations of wear debris obtained during polymer/steel sliding experiments. The results of two separate experimental programs carried out at Virginia Polytechnic Institute and State University were used. Warren [24] observed polymer transfer to rough, ground surfaces; and the author observed polymer transfer to a deterministic surface.

Warren, using OCT, predicted a plane of maximum shear stress in the bulk polymer during the relative sliding of polymer and steel. He hypothesized that the polymer would fracture along this plane, shown schematically in Fig. 6, resulting in a wear particle. The position of this plane of maximum shear stress is described by ϕ, designated the polymer shear angle. Warren attempted to confirm his predicted shear angles through a series of experiments. Although Warren's experiments failed to confirm his predicted shear angles, his observations and measured shear angles are valuable in further model development.

In his experiments conical pins of PVC, PCTFE, and Nylon 6-6 were traversed across a ground steel surface. Each experiment involved a single traverse in a direction perpendicular to the lay of the ground surface. Normal loads of 2.45 N, 9.8 N, and 14.7 N were used

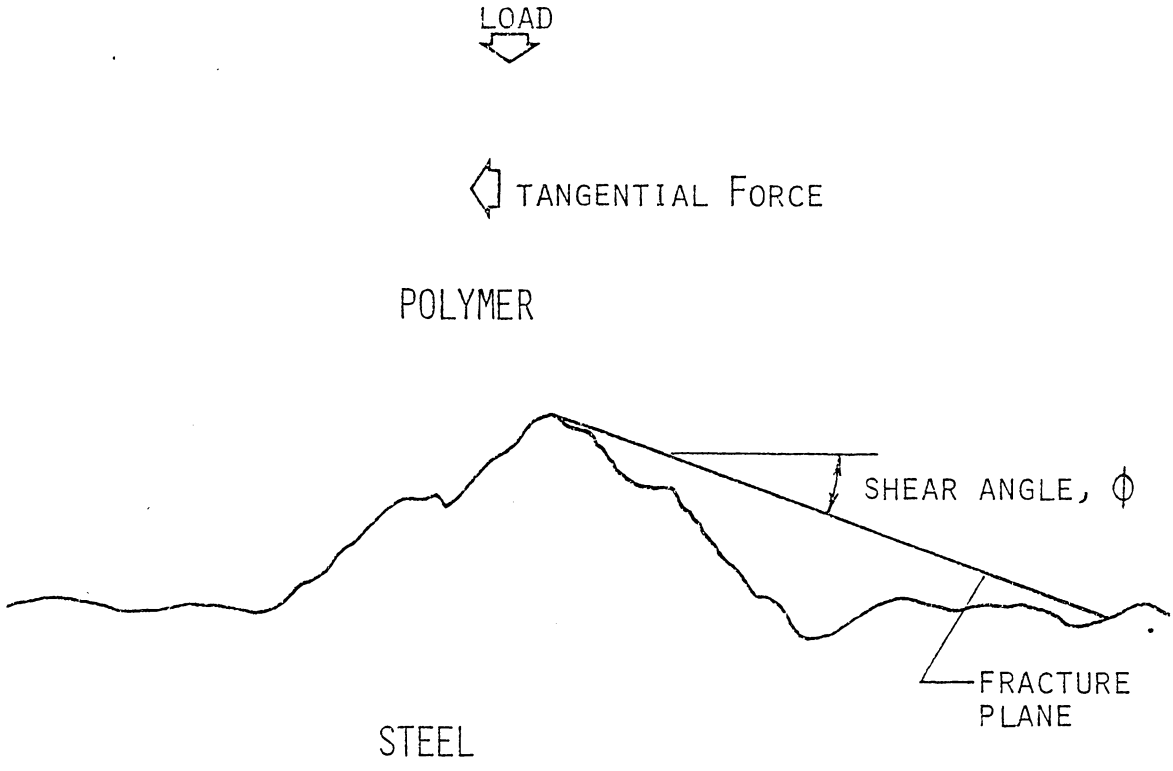

Figure 6. Warren's polymer shear angle [24].

to detect any load dependence of shear angles. When the normal loads were applied to the sharp conical pins, the pins deformed plastically until adequate real area was developed to support the load. Thus the real and apparent areas were equal, providing a BAR equal to one, a condition referred to as full penetration.

Photographs of the polymer deposits were obtained through the use of an AMR 900 scanning electron microscope (abbreviated SEM). The ground surface was positioned in the SEM so that it was viewed as shown in Fig. 7. The angle of view in the photographs is nineteen degrees above the horizon of the surface. This angle was chosen to provide a compromise between the ability to measure polymer shear angles (requiring low elevation angles) and to obtain photographs with the entire field of view in adequate focus (requiring large elevation angles, optimally ninety degrees). As shown in Fig. 7 this low angle of view results in a foreshortening of dimensions in the direction parallel to the grinding lay, resulting in a distortion of the deposits and ground surfaces photographed. Since the SEM has an extremely large depth of field, the foreshortening is not obvious in the photographs. However, when interpreting the photographs, the viewer must remember that foreshortening is present.

Using many such photographs, Warren scaled off and recorded the polymer shear angle. (The author would rather call the angles measured deposit angles, but will defer to Warren's nomenclature.) Since the angles measured from the photographs were not measured in the plane of the surface as shown in Fig. 6, but were instead measured from a nineteen degree elevation, the measured angles were somewhat

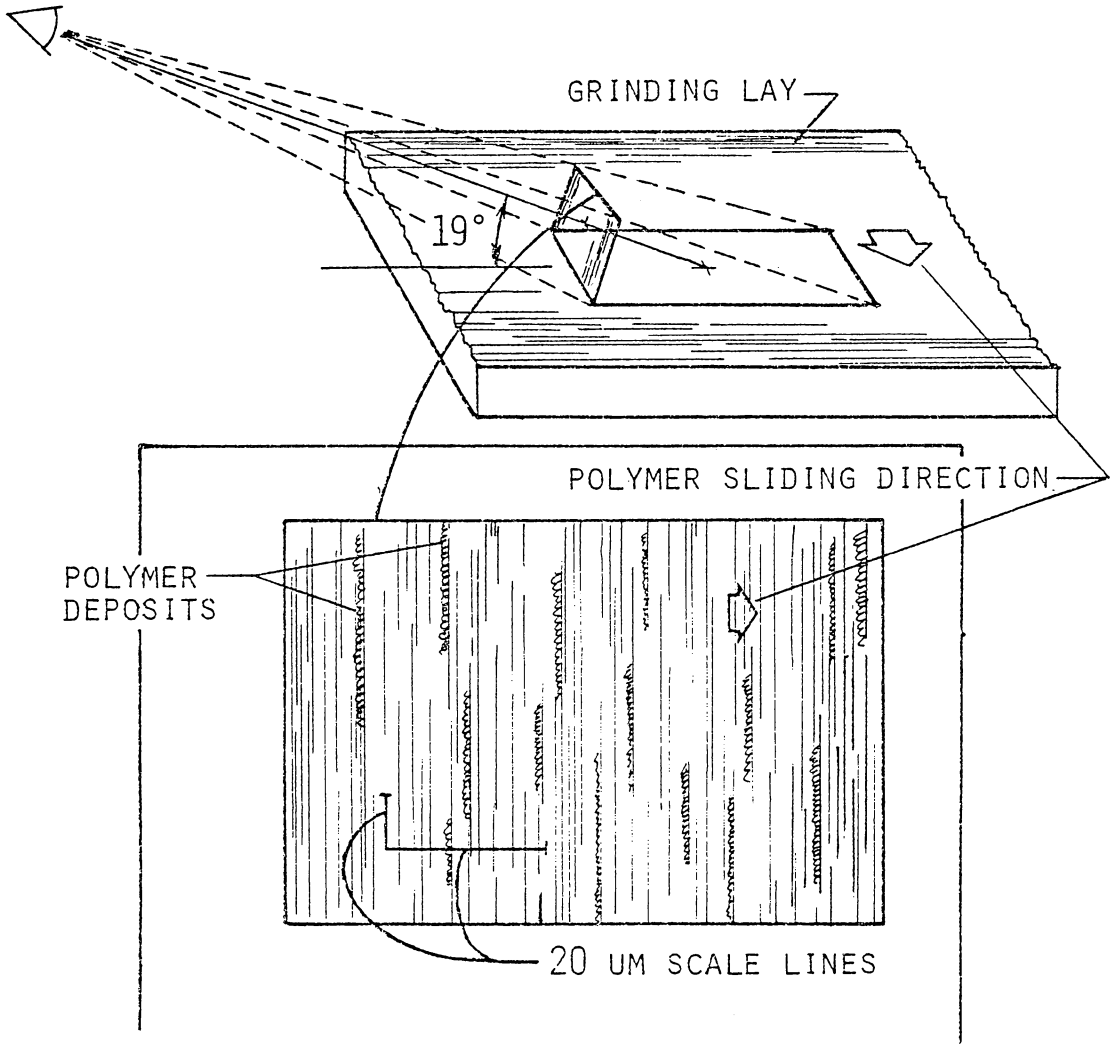

Figure 7. Illustration of foreshortening present in Warren's photographs (Figs. 8-16).

foreshortened also. Warren corrected his measured angles to compensate for this effect. He proceeded to tabulate and to compute statistics for these angles for different polymers and different loads. For a given polymer he found no significant variation of shear angle with load; but between polymers he found significant shear angle variations. Warren found the averaged polymer shear angles to be 18.9° for Nylon 6-6, 12.6° for PCTFE, and 10.8° for PVC.

Several of Warren's photographs are shown in Figs. 8-16 to illustrate typical polymer wear, and to illustrate, in Figs. 10, 11, 13, 14, and 15, typical shear angle measurements as made by Warren. In these photographs the vertical features are the grinding lay. Figures 8-11 are of Nylon 6-6; Figs. 12-14 are of PVC; and Figs. 15 and 16 are of PCTFE transfer. One notes that generally the polymer deposits, dark in color, occur on the leading side of the steel asperities; although occasionally the polymer appears to have flowed over the asperity before being fully released. The reader is referred to Warren's work [24] for a more detailed description and analysis of this work. Of primary interest to this model development is Warren's observation and tabulation of shear angles for these polymers.

The author devised an experimental procedure which would help to illuminate Warren's results. This procedure involved the sliding of six polymers: PVC, PCTFE, Nylon 6-6, LDPE (low density PE), PTFE, and POM, across a deterministic surface. It was decided that the surface was to be of a triangular form with 45° flank angles as shown in cross section in Fig. 17. The surface was made up of 200 sheets of 25.4 μm thick stainless steel which were clamped to the appropriate angle in an

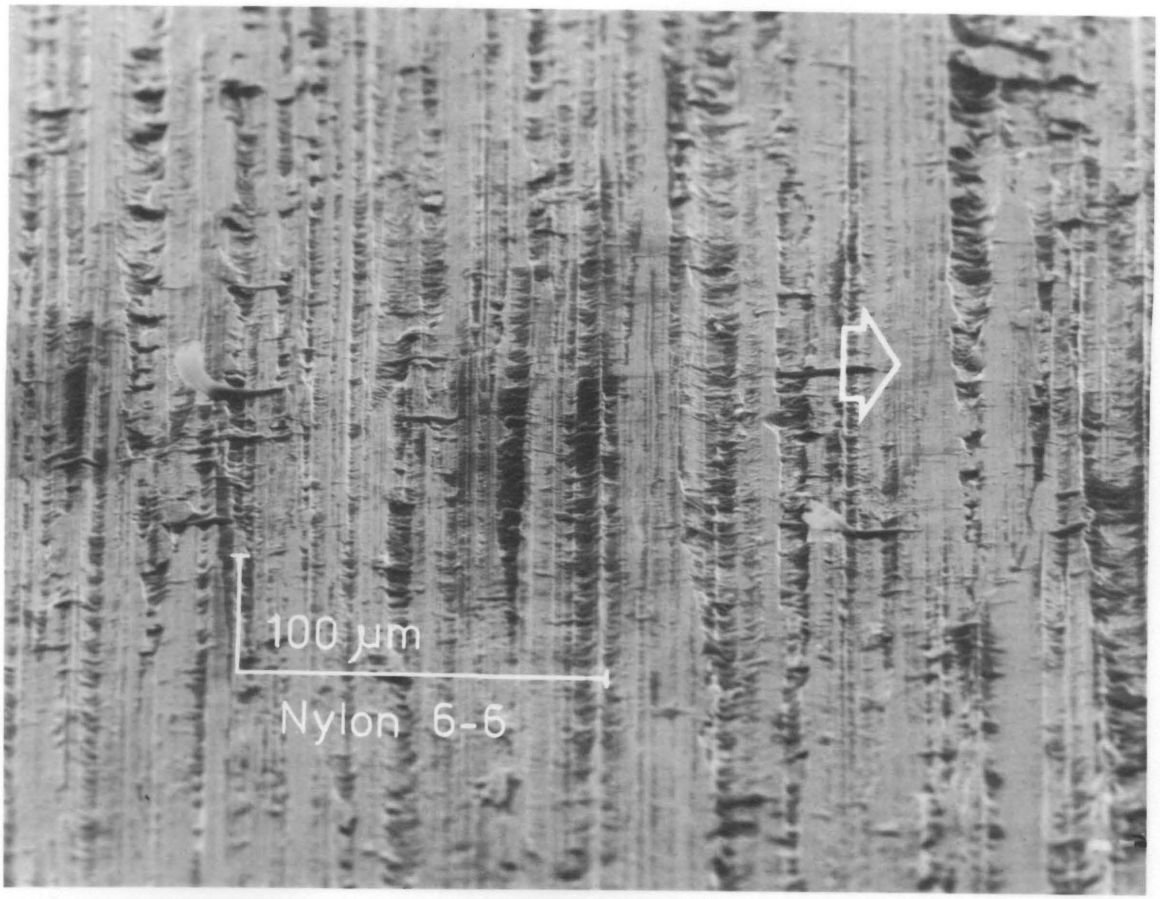

Figure 8. Conical Nylon 6-6 pin run on rectangular block 4, 14.7 N load, 1 Pass, 5/21/76 after Warren [24].

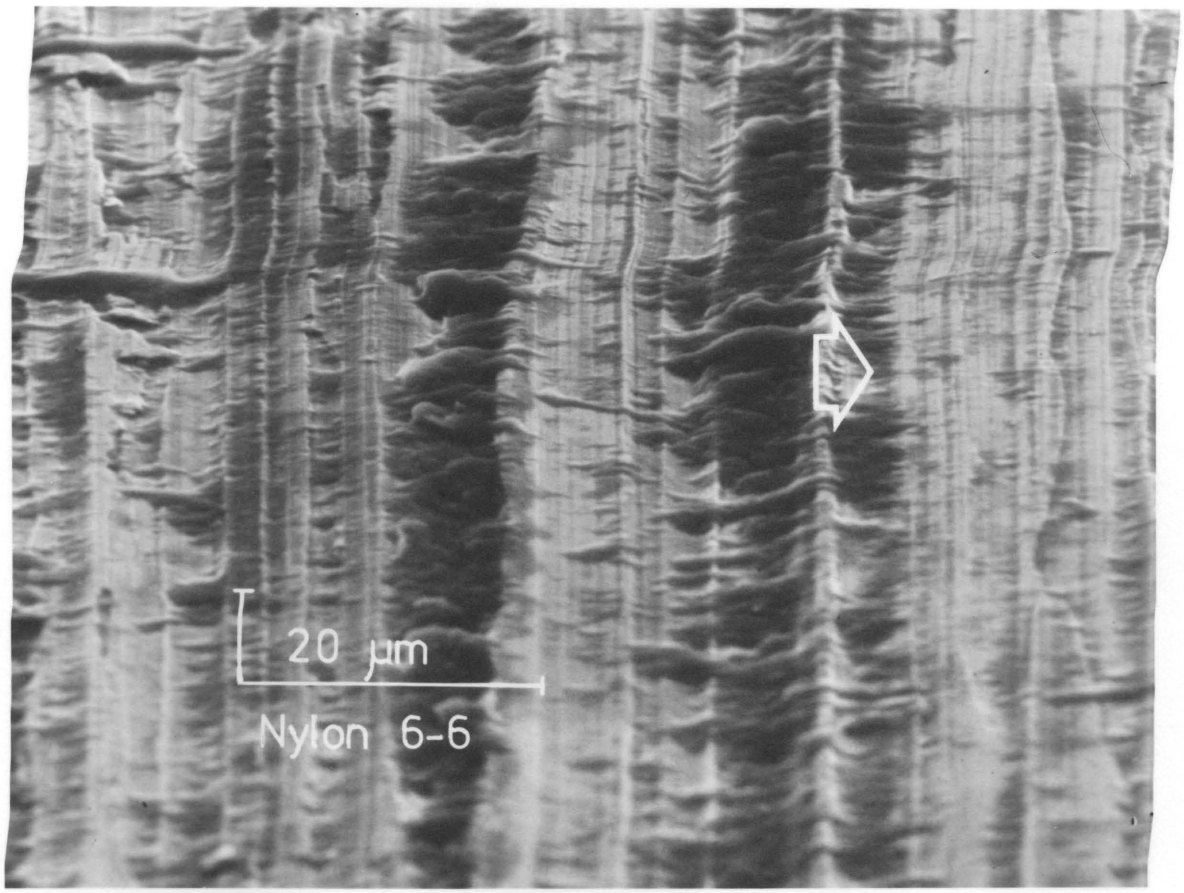

Figure 9. Conical Nylon 6-6 pin run on rectangular block 4, 14.7 N load, 1 Pass, 5/21/76 after Warren [24].

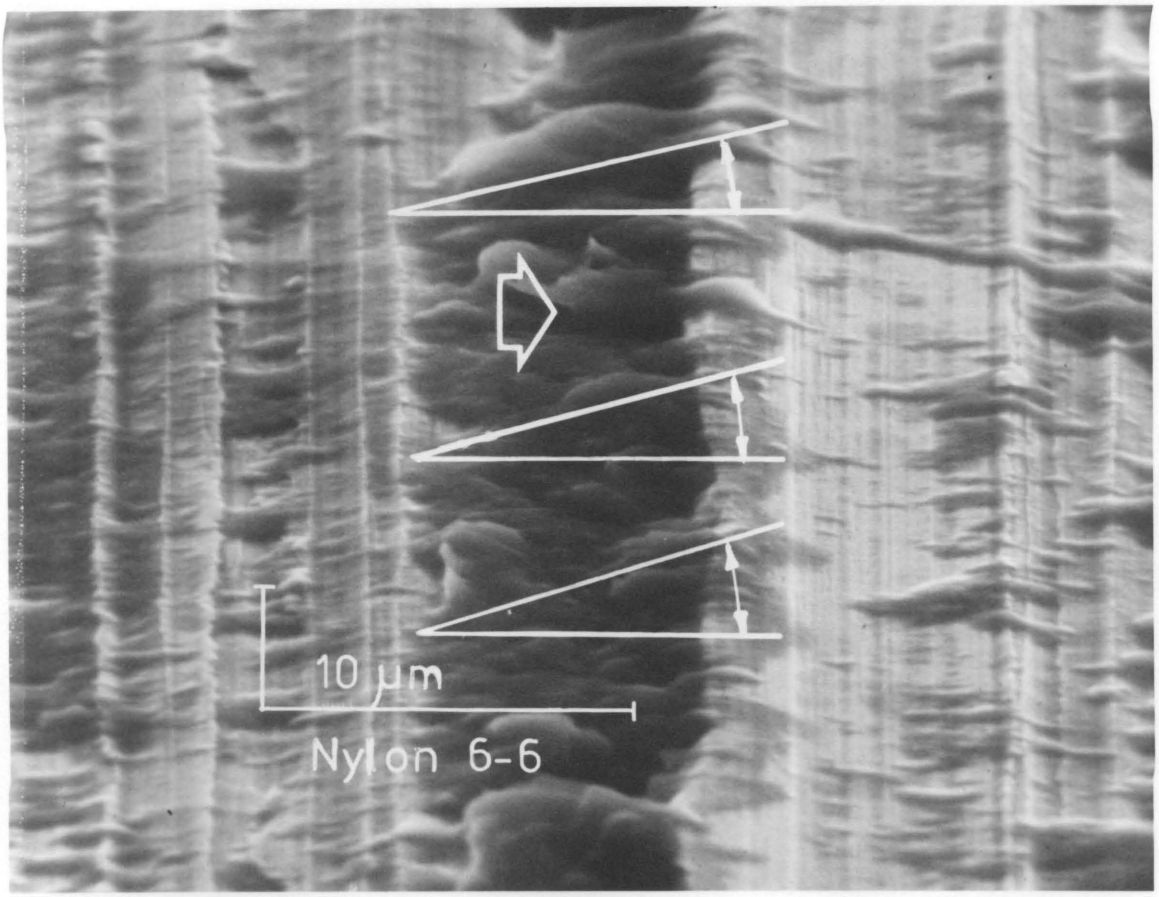

Figure 10. Conical Nylon 6-6 pin run on rectangular block 4, 14.7 N load, 1 Pass, 5/21/76 after Warren [24].

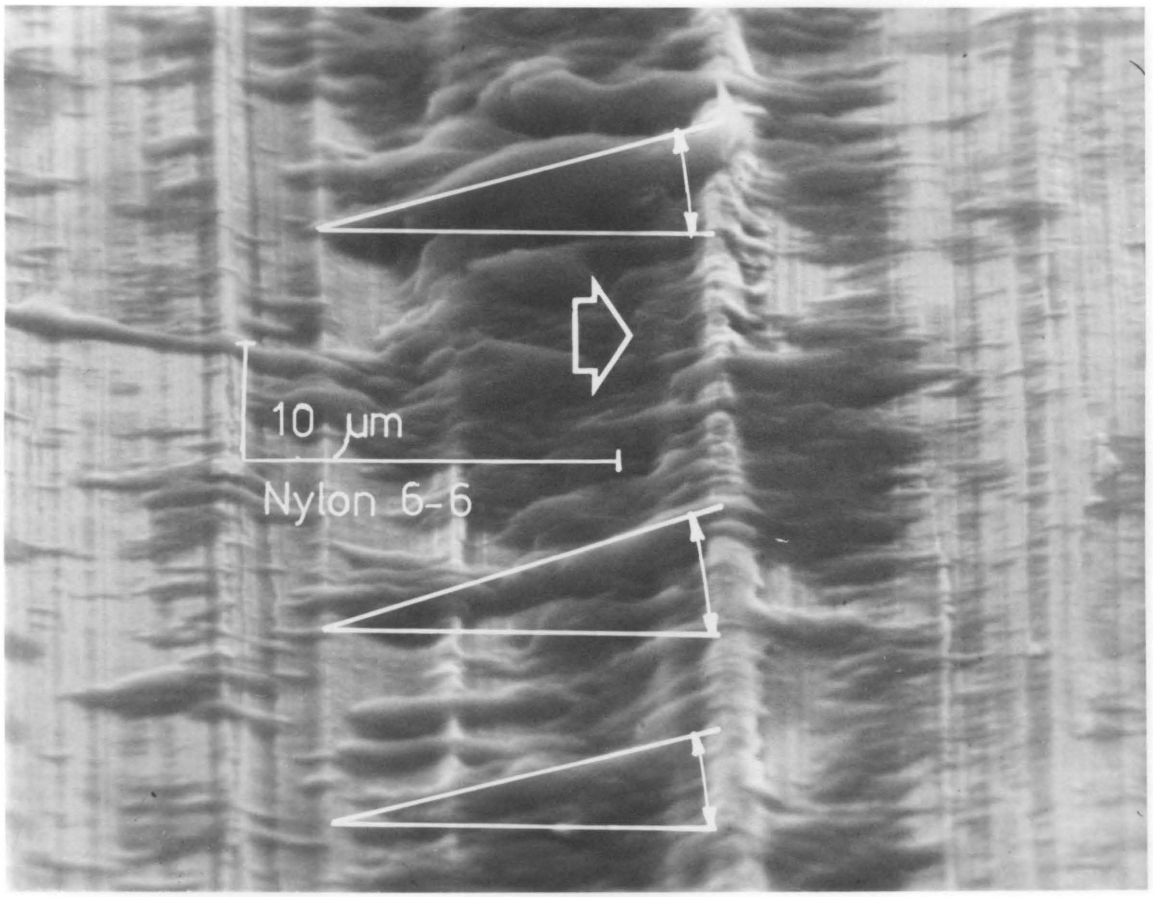

Figure 11. Conical Nylon 6-6 pin run on rectangular block 4, 14.7 N load, 1 Pass, 5/21/76 after Warren [24].

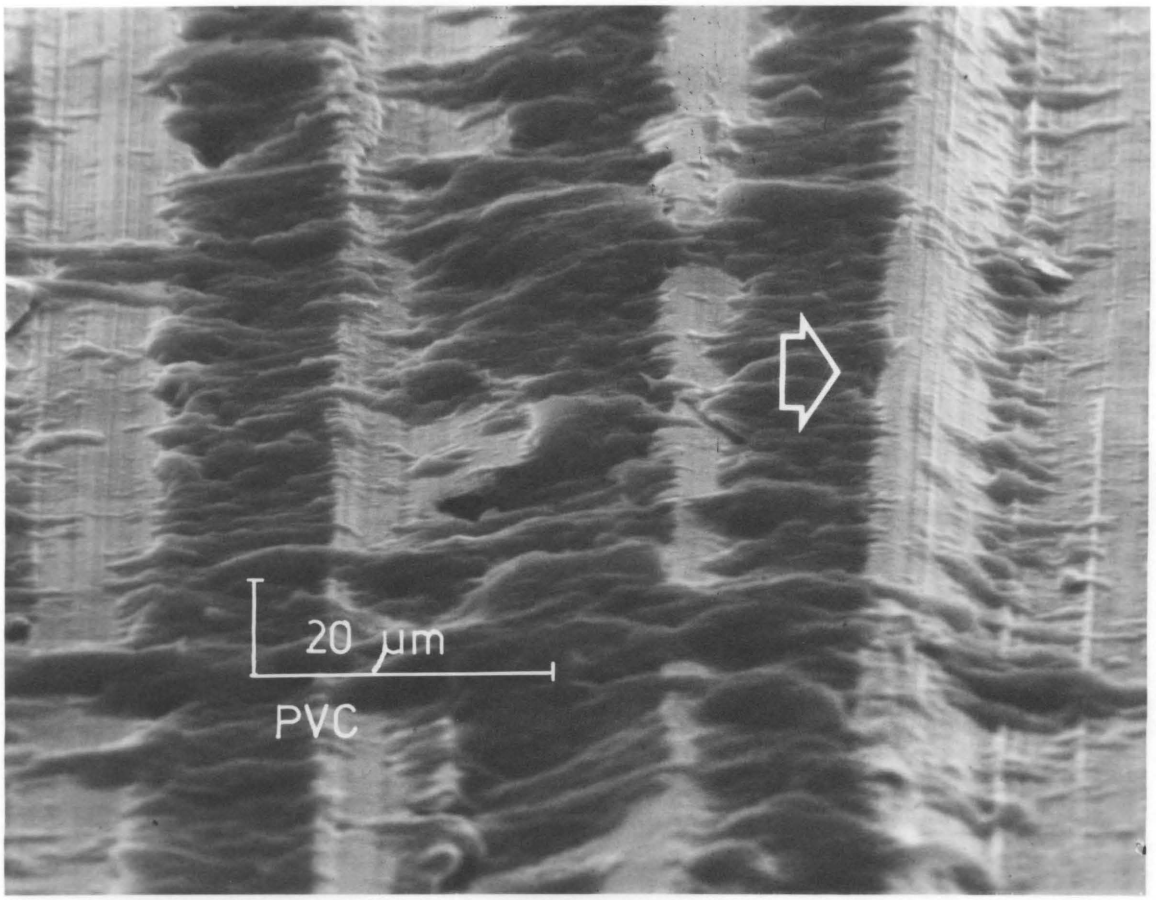

Figure 12. Conical PVC pin run on rectangular block 5, 9.8 N load, 1 Pass, 6/3/76 after Warren [24].

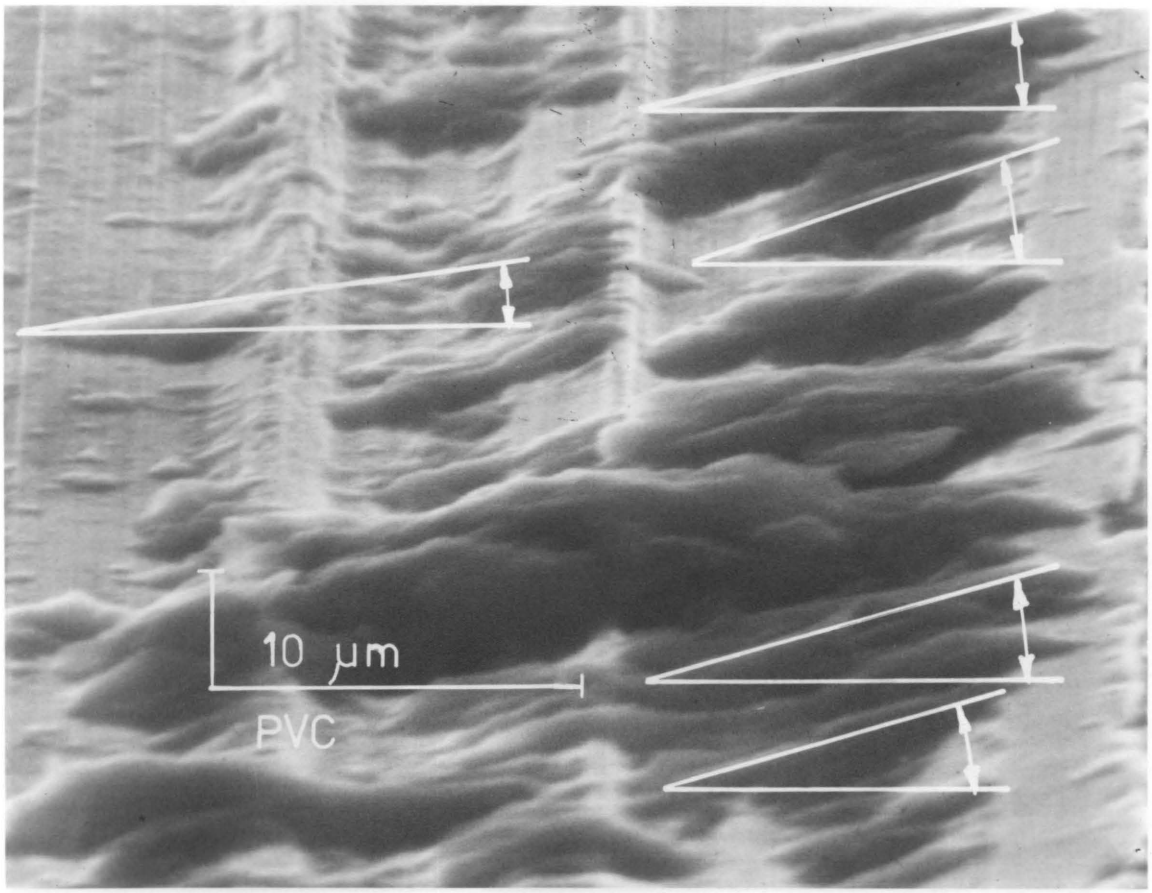

Figure 13. Conical PVC pin run on rectangular block 5, 9.8 N load, 1 Pass, 6/3/76 after Warren [24].

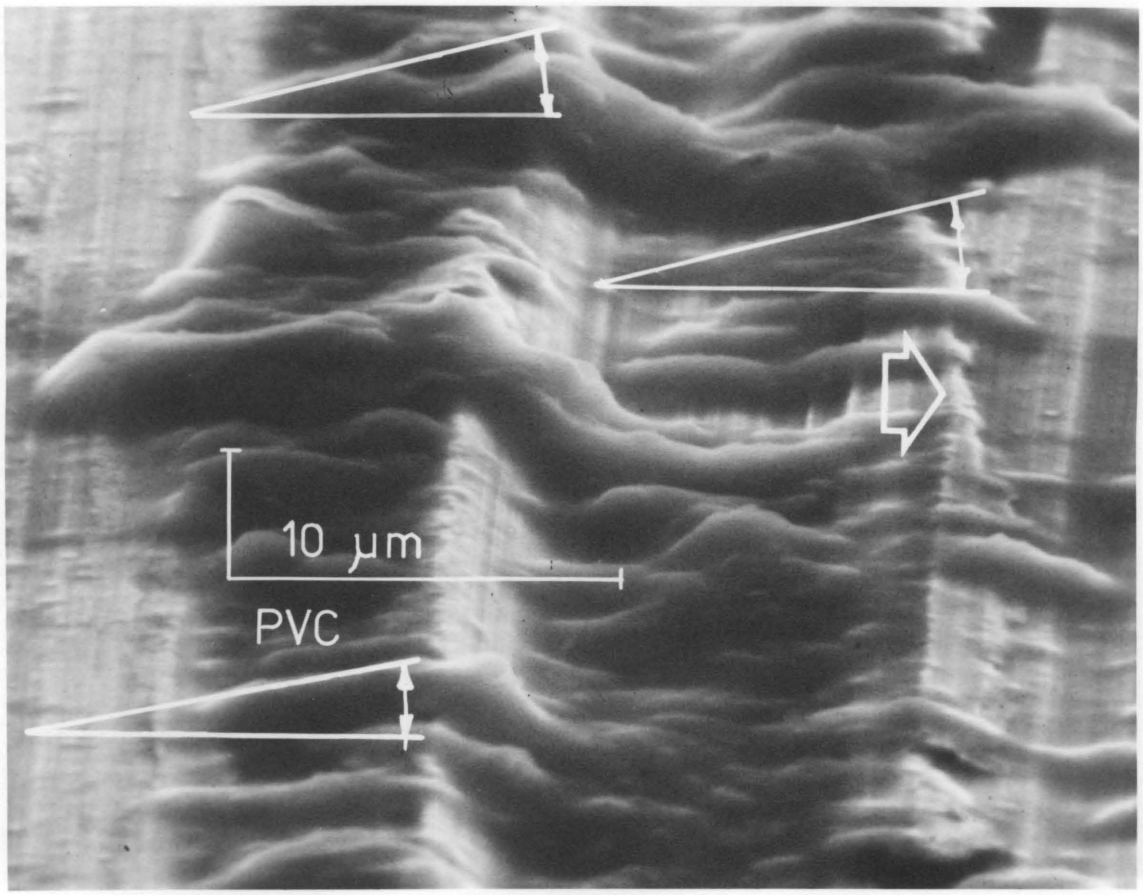

Figure 14. Conical PVC pin run on rectangular block 5, 9.8 N load, 1 Pass, 6/8/76 after Warren [24].

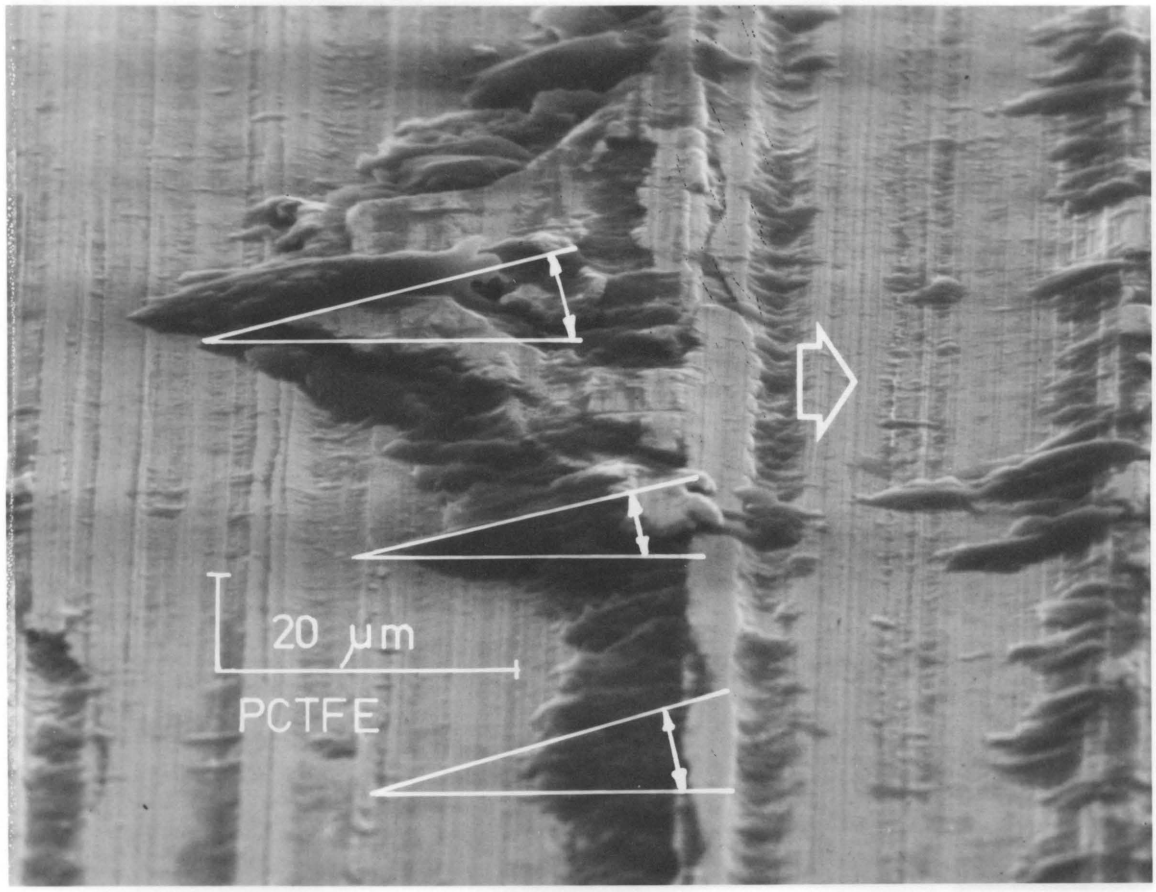

Figure 15. Conical PCTFE pin run on rectangular block 3, 14.7 N load, 1 Pass, 5/19/76 after Warren [24].

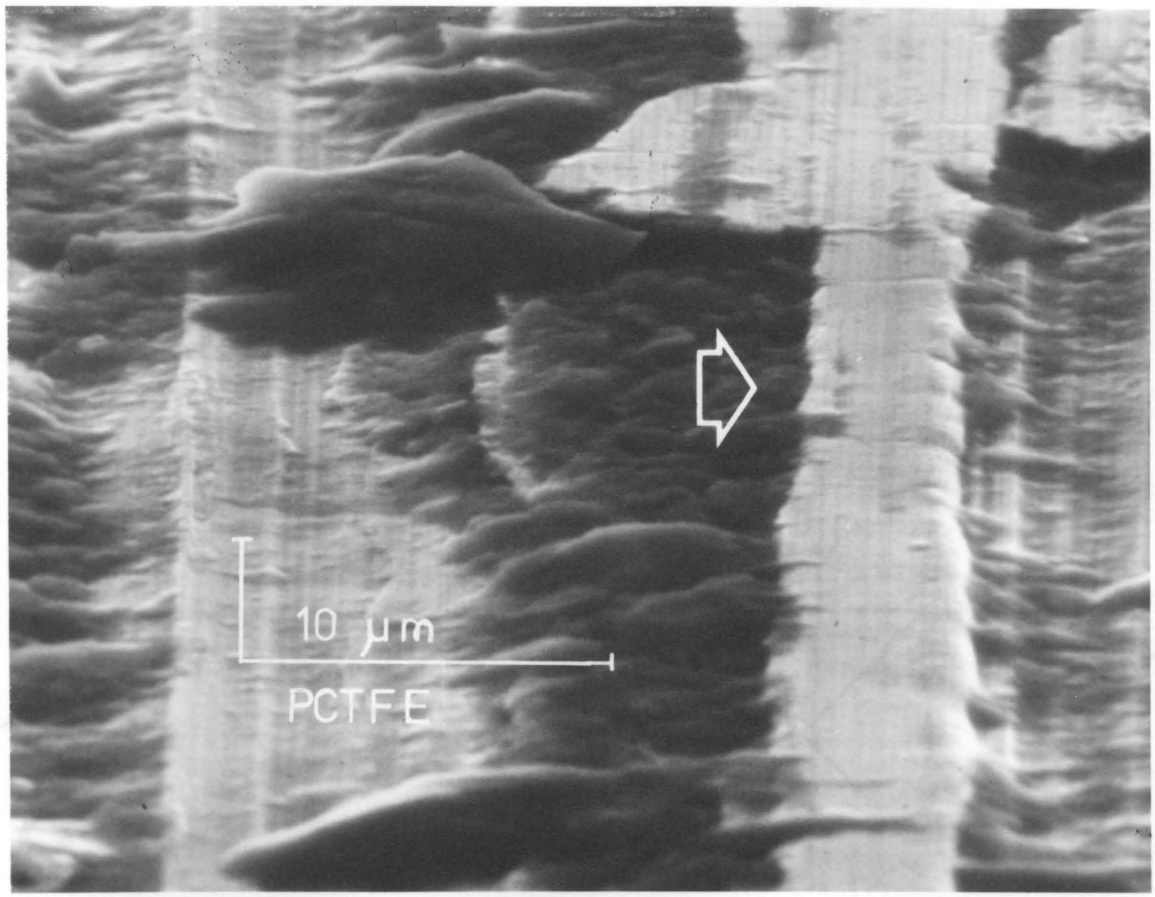

Figure 16. Conical PCTFE pin run on rectangular block 3, 14.7 N load, 1 Pass, 5/19/76 after Warren [24].

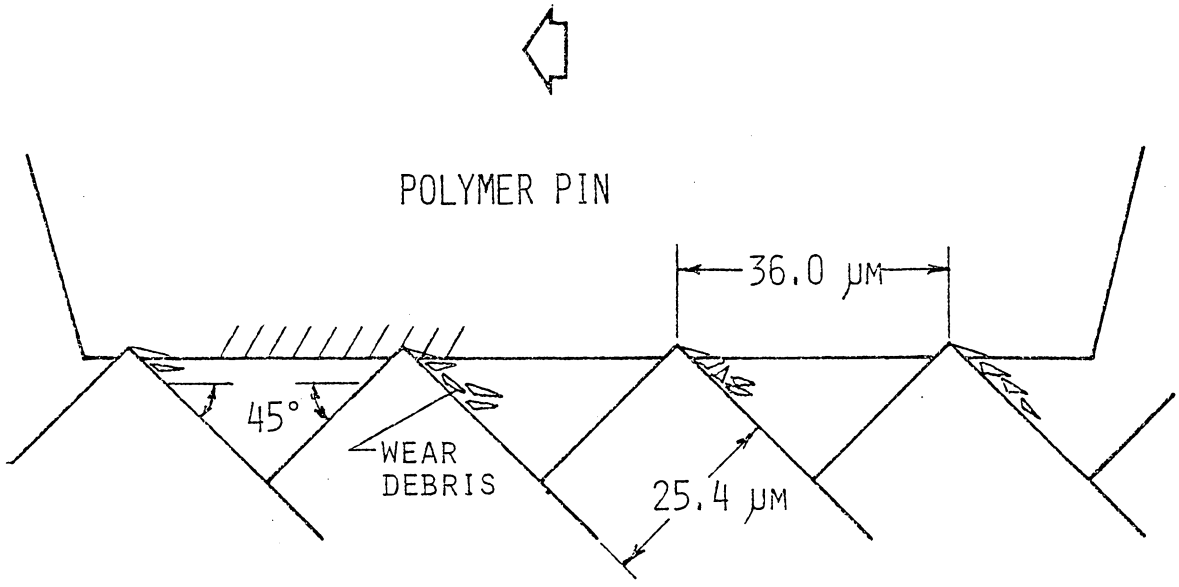

Figure 17. Cross sectional diagram of deterministic surface.

apparatus. As shown in Fig. 17 this geometry provided a peak-to-peak spacing of 36 μm. This surface had an arithmetic average roughness, R_a, of 4.5 μm. The author had desired a surface whose features were on the scale of a ground surface. Although the surface used was somewhat rougher that most ground surfaces, it was felt that this surface would demonstrate wear behavior similar to that of a ground surface. Through the use of this surface, all asperity-to-asperity differences were eliminated if the polymer is assumed to be flat. This isolates any intrinsic variance in the wear process. The polymer pins, in the form of truncated cones, were traversed at approximately 1.0 cm/min across this surface with normal loads calculated to result in a BAR ≈0.1.

All the experiments were carried out under ambient laboratory conditions, the ambient temperature being about 24° C. At this temperature, PVC, PCTFE, and Nylon 6-6 were well below their respective glass transition temperatures, T_g (given in Table 1), a state referred to as glassy. PTFE, LDPE, and POM were tested above their respective T_g's.

Figures 18-23 are SEM photographs of the polymer deposits on the surface, each photograph representing one of the six polymers. The three polymers tested at temperatures below their T_g's, shown in Figs. 18, 19, and 20, all exhibit the similar phenomenon of discrete, uniform sized wear debris. The Nylon 6-6 debris of Fig. 20 is a particularly good example of the discrete polymer wear process which this author has found to be characteristic of the wear of glassy polymers, those polymers below their T_g. The top of this photograph represents the region near the edge of the polymer pin prior to sliding. Three discrete lumps,

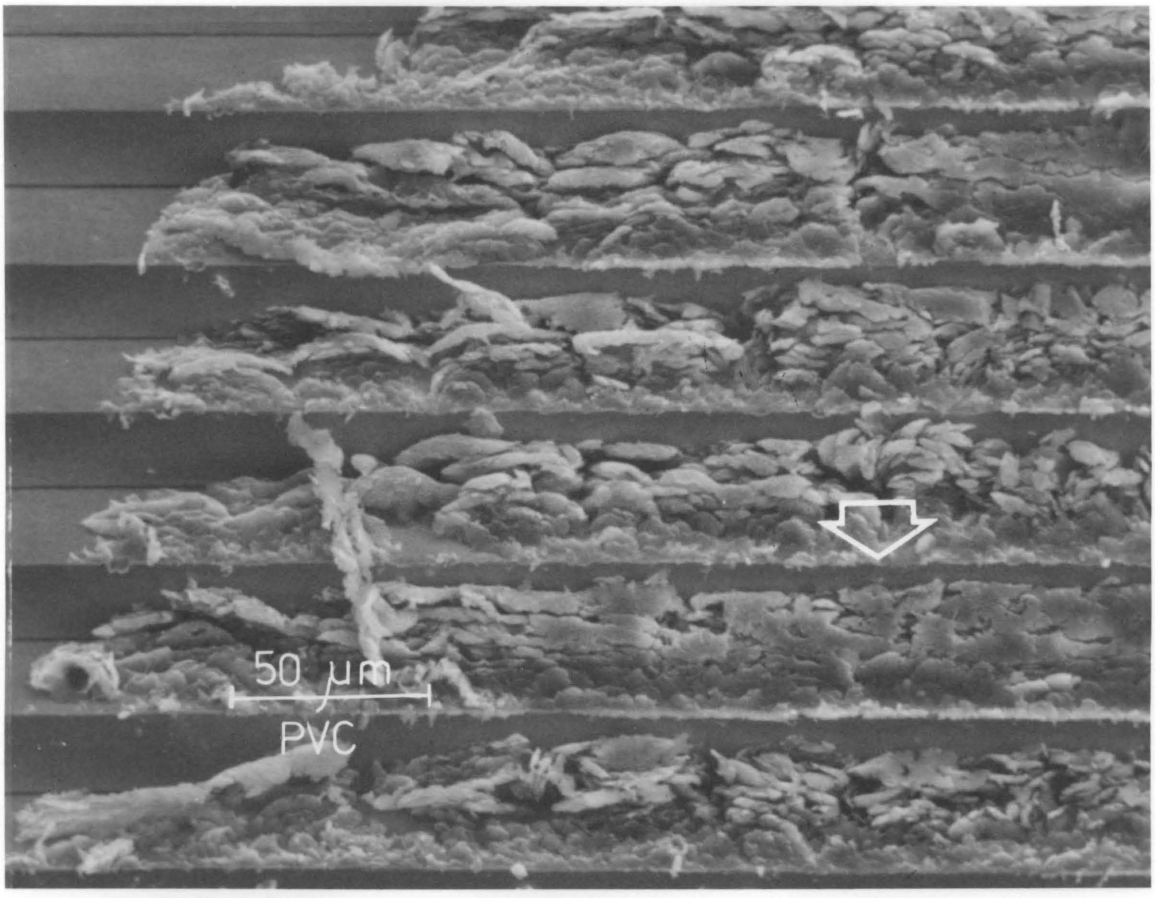

Figure 18. Conical PVC pin run on deterministic surface, BAR=0.1, 1 Pass, 4/2/79.

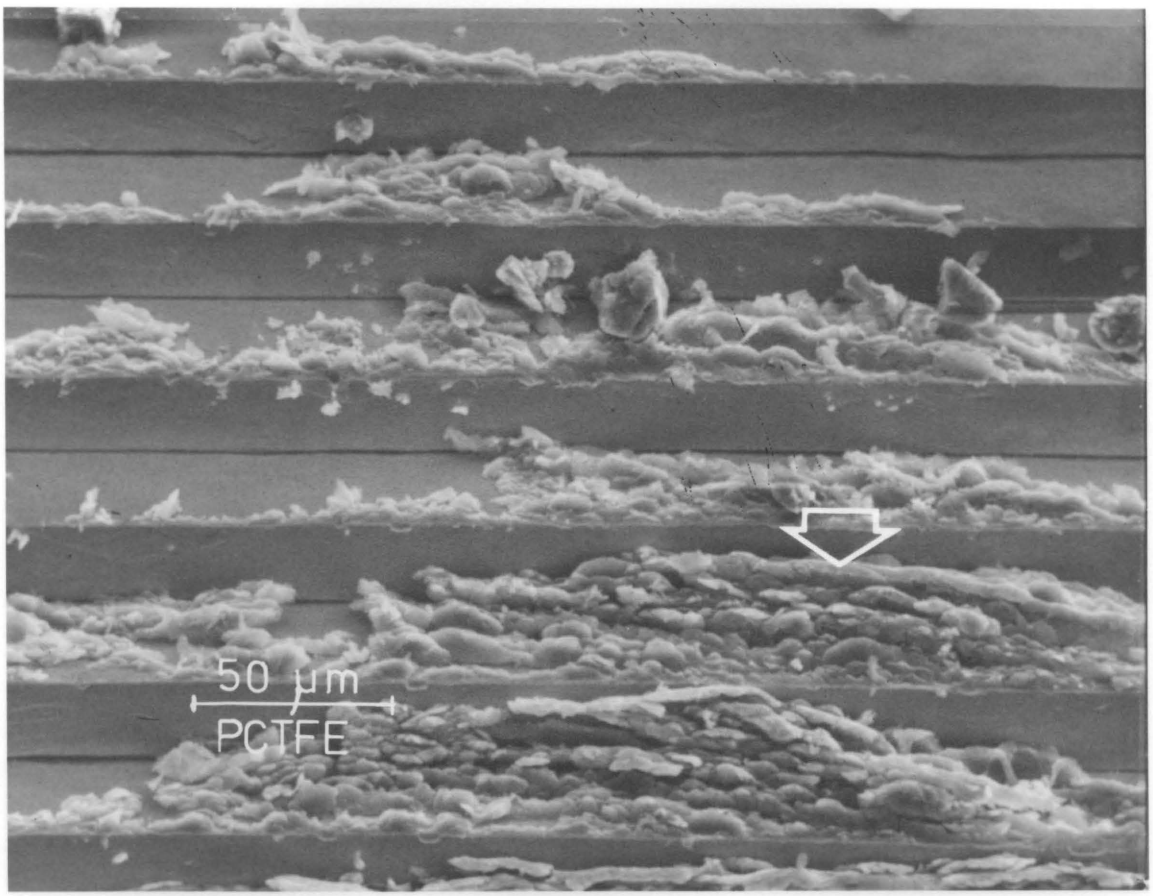

Figure 19. Conical PCTFE pin run on deterministic surface, BAR=0.1, 1 Pass, 4/2/79.

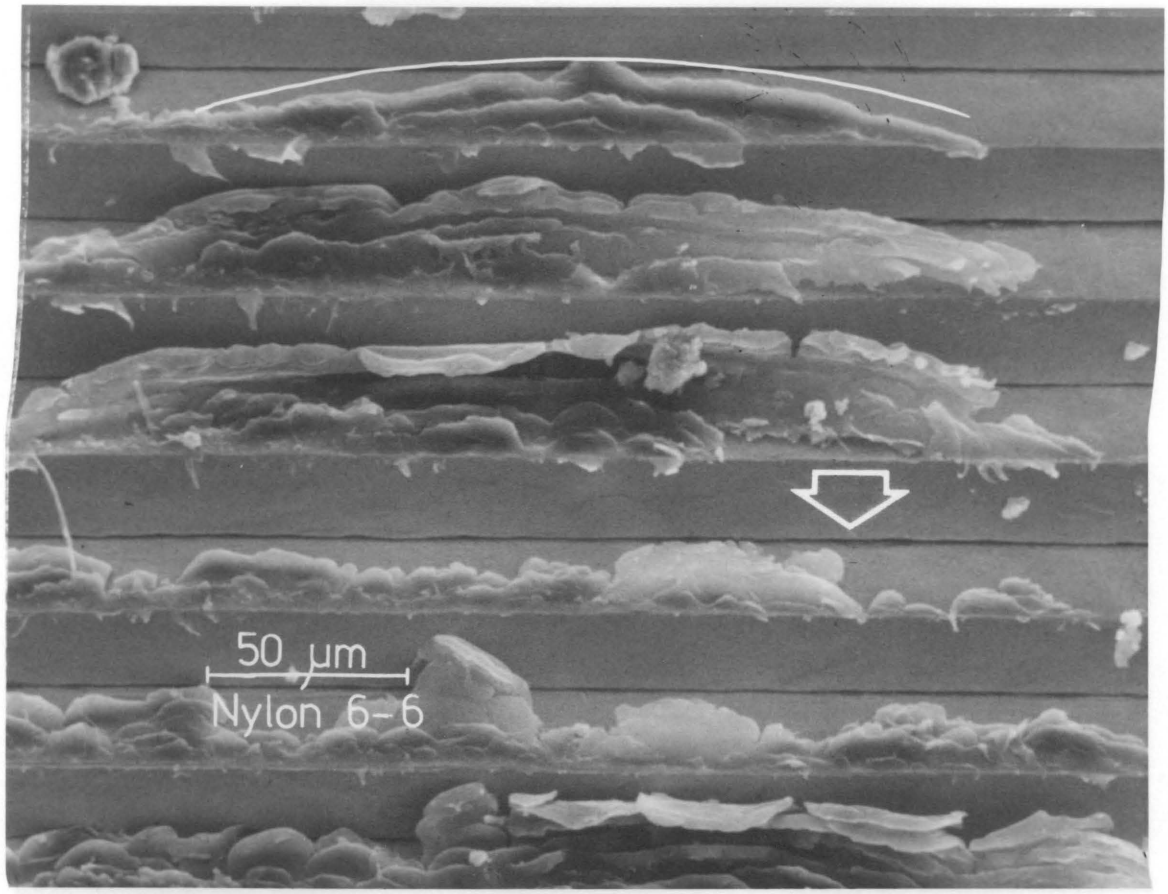

Figure 20. Conical Nylon 6-6 pin run on deterministic surface, BAR=0.1, 1 Pass, 4/2/79. Sketched arc represents the initial position of the circular contact area prior to sliding.

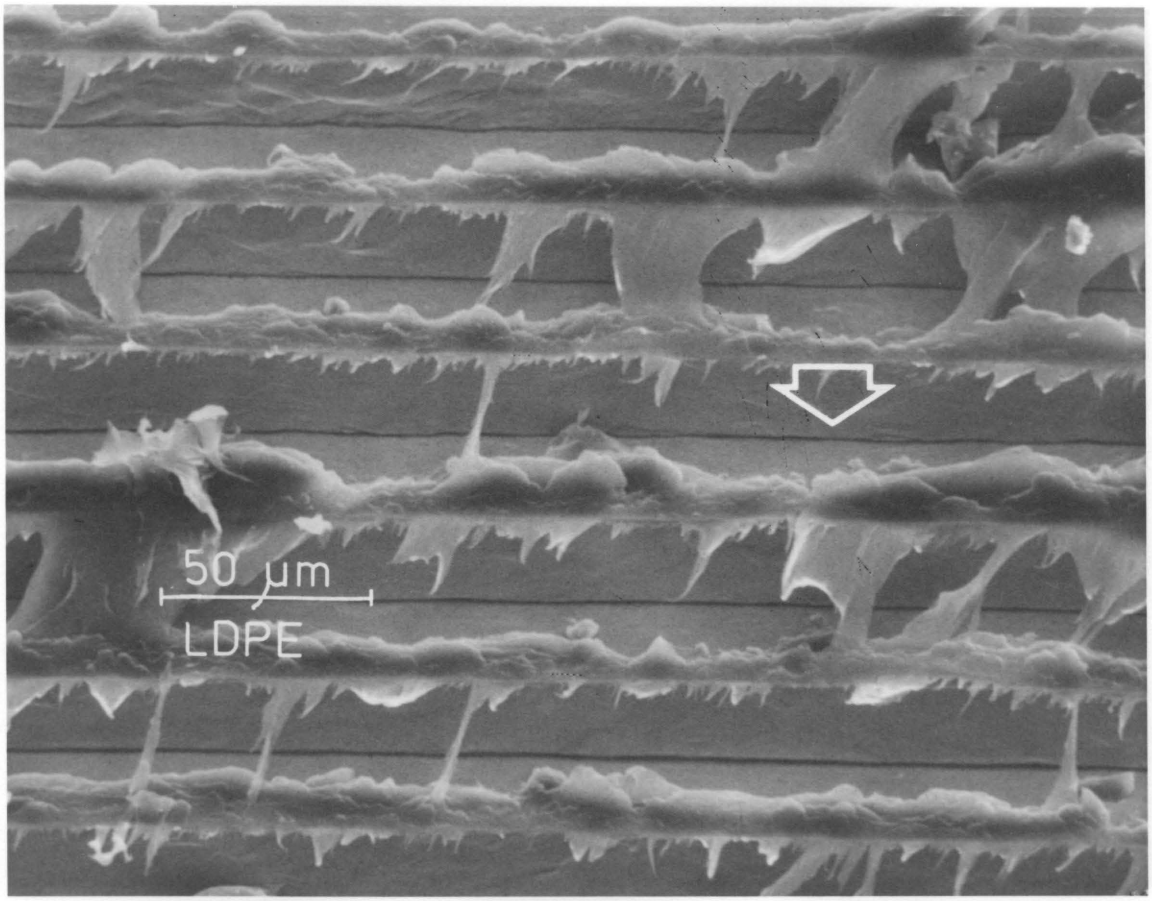

Figure 21. Conical LDPE pin run on deterministic surface, BAR=0.1, 1 Pass, 4/2/79.

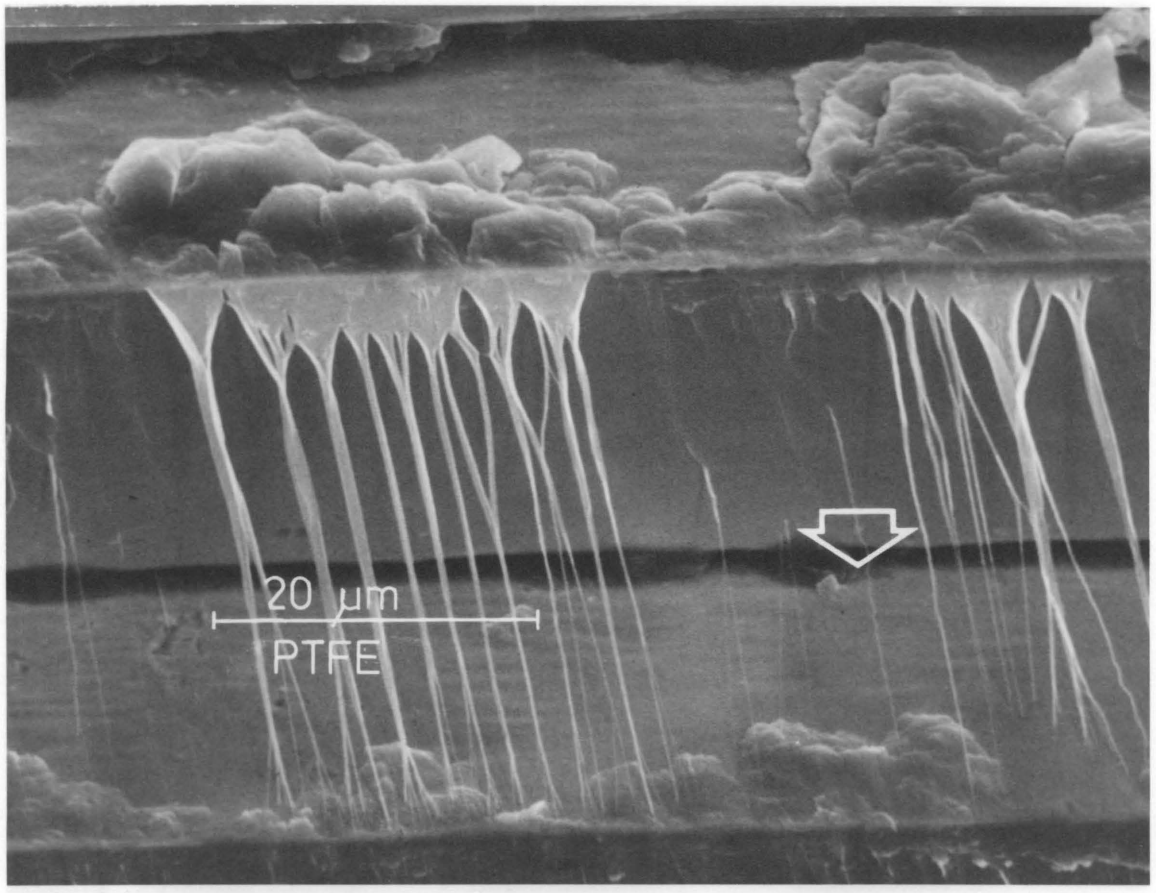

Figure 22. Conical PTFE pin run on deterministic surface, BAR=0.1, 1 Pass, 4/6/79.

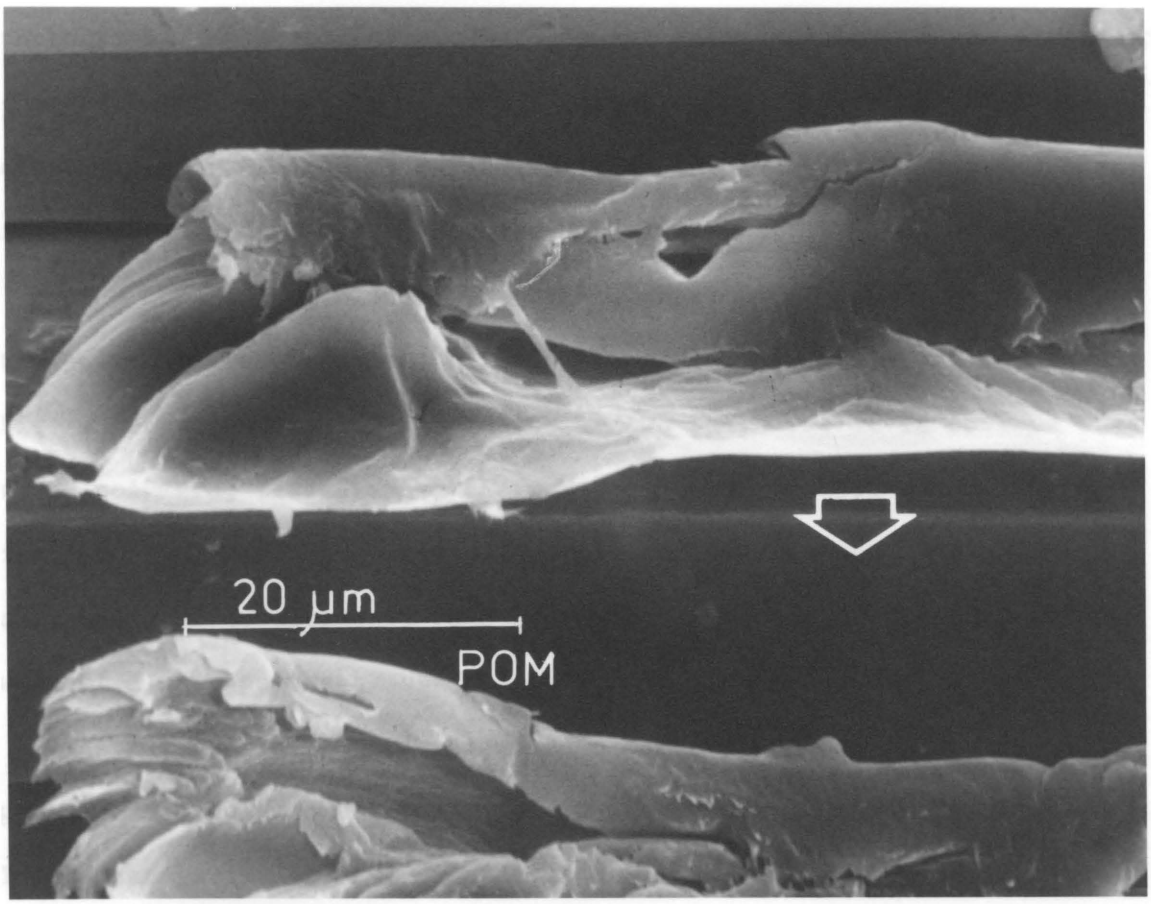

Figure 23. Conical POM pin run on deterministic surface, BAR=0.1, 1 Pass, 4/6/79.

or wedges, of material can be seen in the valley at the top of the photograph. Each is shorter that the one below because of the diminishing chordal length of the circular pin as one approaches the edge of the circular apparent area of contact. It is this wear in discrete lumps, idealized as wedges, that this wear model will attempt to simulate.

The LDPE of Fig. 21 and the PTFE of Fig. 22 exhibit drawing of the polymer into sheets and strands respectively. While the POM of Fig. 23 does not draw as do the former two polymers, it is obvious that these polymers, tested above their T_g's, do not exhibit the characteristic mode of wear of glassy polymers. For this reason, the model of abrasive wear developed in this dissertation is applicable only to the wear of glassy polymers.

As a result of the aforementioned observations of the wear debris generated in polymer/steel sliding, a wedge model for debris was used. These wear particles were modeled as shown in Fig. 24. There are two necessary conditions for the generation of wear debris. First, the asperity must penetrate the polymer. Second, of that portion penetrating the polymer, the cutting side must have an angle, γ, greater than the shear angle, ϕ, for the polymer. Figure 24a, b, and c shows various permutations of asperity geometries, and how they were considered to behave in a sliding application.

This assumed geometry of wear displays several characteristics deemed fundamental to abrasive polymer wear:

a) Obviously, an asperity must at least penetrate the polymer before it can be considered as a possible cutting asperity (ref. Fig. 24a)

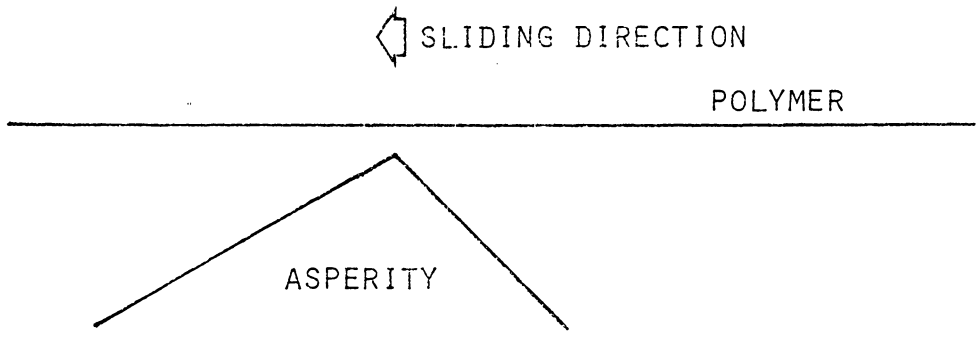

A) ASPERITY NOT A CUTTER DUE TO FAILURE TO PENETRATE POLYMER.

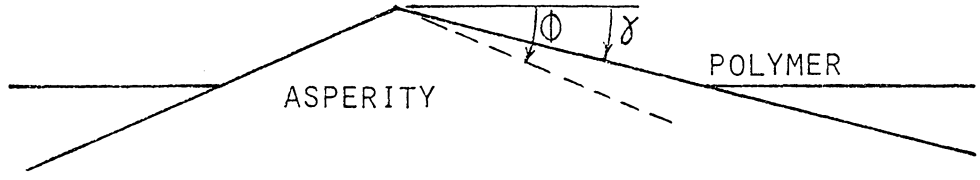

B) ASPERITY NOT A CUTTER DUE TO A TOO SMALL SLOPE, $\gamma < \phi$

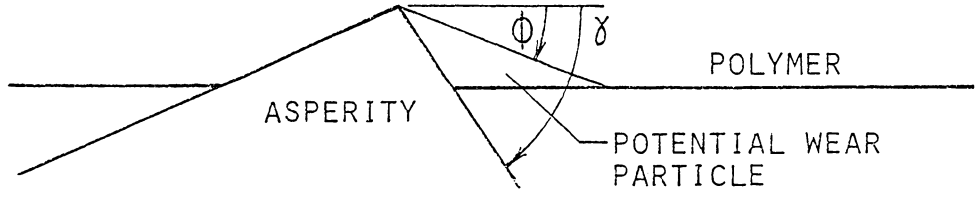

C) ASPERITY IS A CUTTER, $\gamma > \phi$

Figure 24. Possible asperity/polymer interactions: a) no asperity penetration, b) asperity penetrates but does not cut, $\gamma \leq \phi$, and c) asperity penetrates and cuts, $\gamma \geq \phi$.

b) An asperity which penetrates the polymer must have a slope at least as large as the shear angle; otherwise, it is too blunt and will not result in wear (ref. Fig. 24b).

c) Given that an asperity penetrates the polymer and has a slope greater than the shear angle, greater slopes will result in increasingly greater wear (ref. Fig. 24c).

3.4. Wear Particle Formation Rate

The previous section detailed the shape and geometry of modeled wear particles. This section concludes the fundamental model development with a discussion of the rate of wear particle formation.

The asperities shown in Fig. 24 are oversimplified in that they are shown with but one slope on each side. In fact, asperities almost never have these constant flank angles, but instead have continuously varying flank angles. Figure 25 shows an asperity with a continuously varying flank angle, and the model of a potential wear particle. Hereafter, the term "asperity encountered material" is taken to be a layer of polymer with a thickness equal to the wedge height at asperity i, WH_i , as shown in Fig. 25.

OCT predicts the removal of a layer of thickness equal to the asperity penetration depth as shown in Fig. 25a. In contrast, the present model uses as its assumed maximum wear the asperity encountered material only. As this layer encounters the asperity during sliding, some of the material in this layer is assumed to be broken free of the bulk polymer as wear particles. The remainder of this layer is assumed to pass over the asperity while undergoing plastic and elastic deformation.

The wear particle formation rate describes the number of wear particles formed per unit sliding distance at any given asperity. This rate, in combination with the wedge area, WA_i , and the wedge height, WH_i , determines the percentage of the asperity encountered material which becomes wear debris. Specifically, the particle formation rate may be no greater than that which results in wear particles which equal 100% of the asperity encountered material.

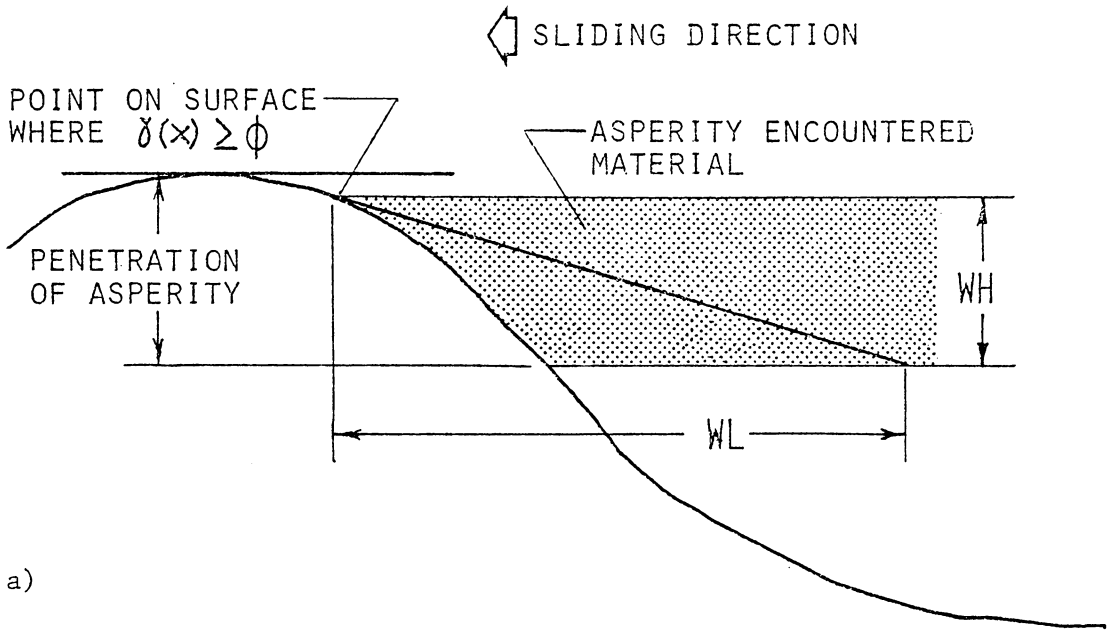

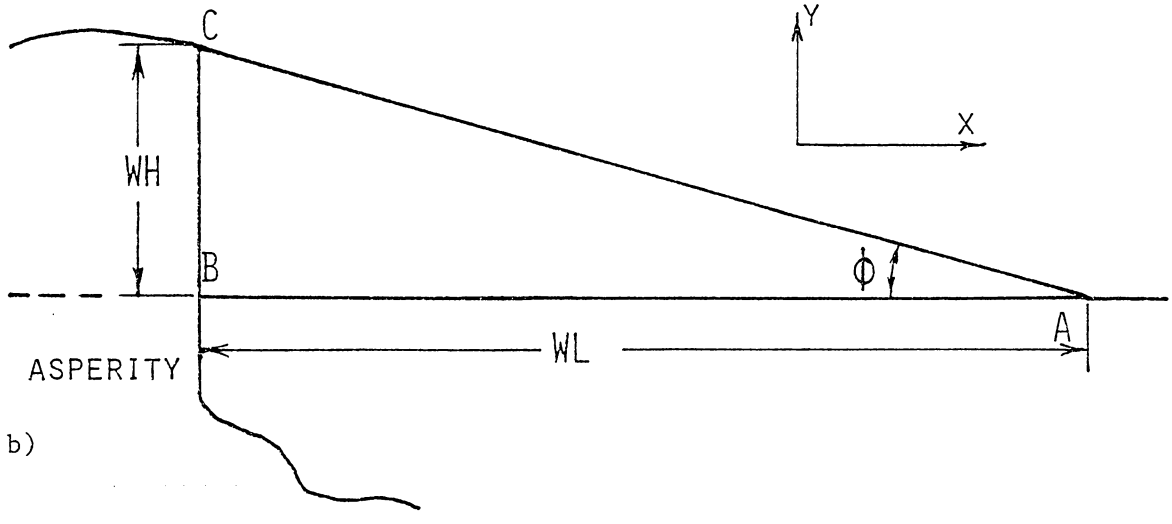

Figure 25. Illustration of: a) asperity encountered material, and b) modeled wedge geometry.

It was assumed that wear particles form at a rate inversely proportional to a multiple of their length. This multiple is specified as the factor G, and is interpreted as follows: When the bulk polymer is slid a distance $G \cdot WL_i$, where WL_i is the wedge length of the modeled wedge at asperity i, the total volume worn at asperity i is assumed to suddenly increase by the volume of the modeled wedge. Since this is a two-dimensional model, the wedge volume and the corresponding available void volume at site i are found as a wedge area, WA_i, and a void area, VA_i, as shown in Fig. 26. The volumes associated with these areas are obtained by multiplying the areas by the slider width.

The effect of the factor G is demonstrated graphically in Fig. 27. For a typical wedge, the particle formation rates corresponding to G = 0.5, 1.0, and 1.5 are shown. It can be seen that increasing values of G are associated with a decreasing percentage of the asperity encountered material being modeled as wear particles.

When this model for the wear particle formation rate is used, the effective continuous wear rate at asperity i is $WA_i/(G \cdot WL_i)$*. The thickness of the asperity encountered material is equal to the wedge height, WH_i, and the continuous wear corresponding to all the asperity encountered material being worn is $(WH_i \cdot WL_i)/WL_i$. The requirement that the simulated wear be no more than the asperity encountered material is expressed in the relation $WA_i/(G \cdot WL_i) \leq (WH_i \cdot WL_i)/WL_i$, which, when solved for allowable values of G, yields

$$G \geq \frac{WA_i}{WL_i \cdot WH_i} \quad . \tag{12}$$

Although in the general case, WA_i, WL_i, and WH_i are independent of

* Wear rate here is defined as the wedge area divided by the sliding distance necessary to produce a wedge. (dimensional units of L^2/L)

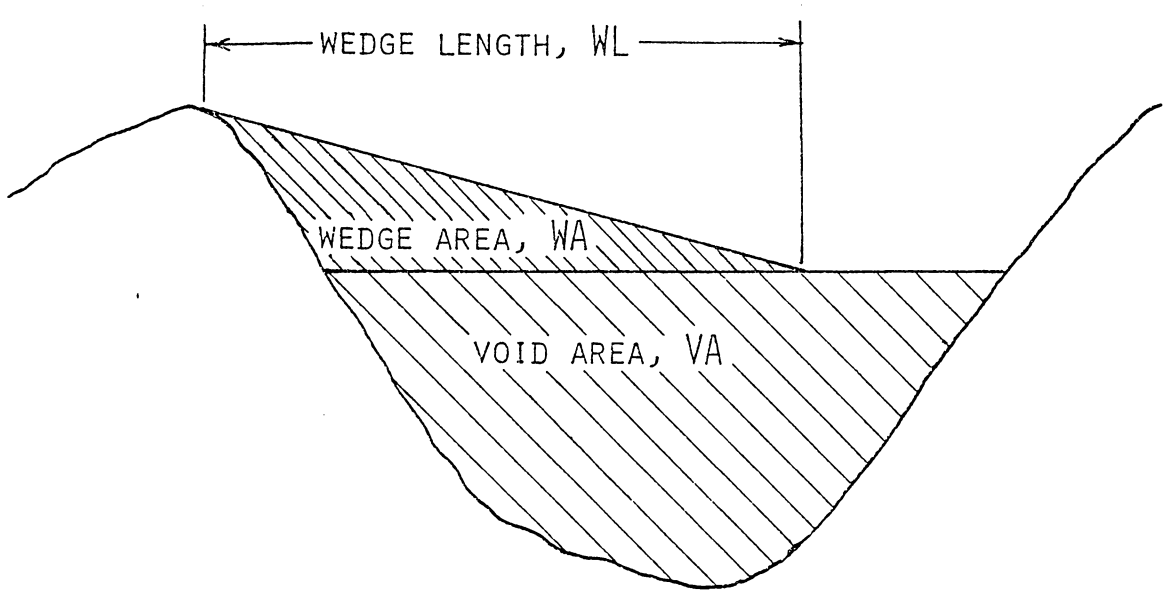

Figure 26. Quantities associated with a modeled wear site.

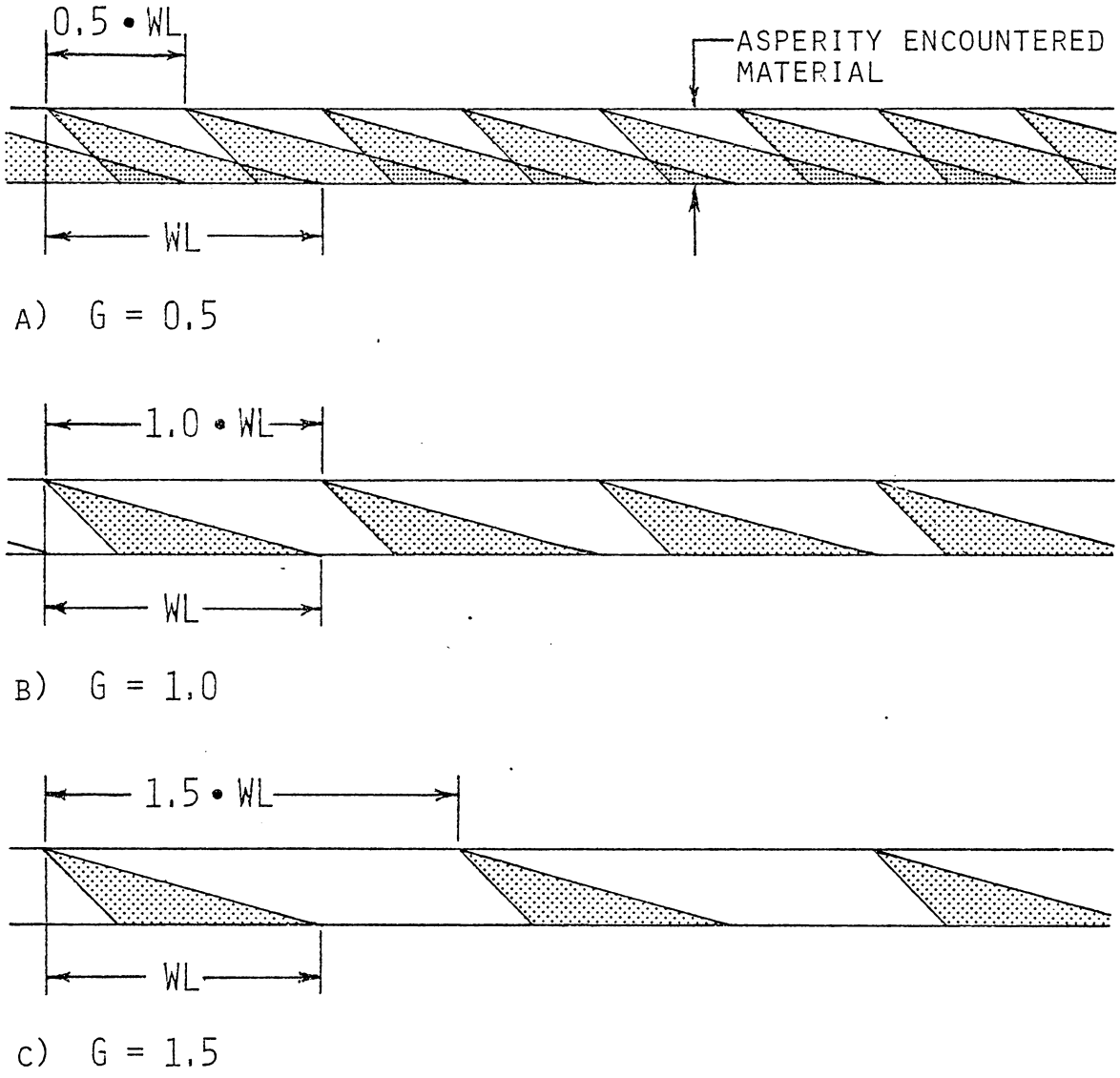

Figure 27. The effect of the factor G on the wear particle formation rate with: a) G = 0.5, b) G = 1.0, and c) G = 1.5 .

each other, a special case of the otherwise arbitrary wedge shape serves to demonstrate the limitation on G implied by Eq. 12.

If one excludes the possibility of a ground surface having a convoluted profile, then the steepest slope, γ, an asperity may have is ninety degrees. (Although the grinding process might produce a convoluted surface, the convolution would not be detectable with the stylus techniques used to obtain profiles for this model.) Such an asperity would produce a wedge modeled as a right triangle, shown in Fig. 25b as the area enclosed by points ABCA, For a given wedge length and wedge height, this configuration results in the largest possible wedge area, given by the relation $WA_i = \frac{1}{2} \cdot WL_i \cdot WH_i$. Upon substitution of this equation for WA_i into Eq. 12, one arrives at the relation

$$G \geq \frac{\frac{1}{2} \cdot WL_i \cdot WH_i}{WL_i \cdot WH_i} = 0.5 \quad . \qquad (13)$$

Since real asperities have slopes less than ninety degrees, the wedge area will always be less than that given by $\frac{1}{2} \cdot WL_i \cdot WH_i$, yielding minimum values of G less than 0.5 . Therefore, if values of $G \geq 0.5$ are used in the model, there is no risk of violating Eq. 12.

The discussion so far has concerned only the theoretical lower limit of G. The question now arises "What value of G should be used in the model?" The factor G is related to the strain the polymer must undergo before a wear particle breaks free of the bulk polymer. Therefore, G is related to the elongation at break, ε, of the polymer being simulated. Dependence of polymer wear on ε has been observed by other researchers. Ratner, Farberova, Radyukevich, and Lur'e [25] state "...the act of wear as a separation of particles occurs only when

the elongation brought about by the abrasion exceeds the breaking elongation of the material..." Lancaster [26] observed a striking correspondence between the temperature dependence of wear and the temperature dependence of the quantity $1/S\varepsilon$, where S is the breaking strength in tension. Although the two dependencies are similar, suggesting a proportionality between wear rate and $1/S\varepsilon$, the temperatures at which these two functions have minima do not compare well. Lancaster speculates that this apparent discrepancy is caused by the uncertainty of strain rates associated with the wear process, combined with the strong influence of strain rate on the measured mechanical properties of polymers.

The factor G might well be taken to be a linear function of ε for a given polymer. However, at this stage of the model development the function is not known. Therefore, it was assumed that $G = 1.0$. In section 4.3., when model predictions are compared with experimental wear data, the value of G will be reexamined with regard to its relationship to ε.

3.5. Computing Environment and Data Acquisition

The model of abrasive polymer wear, as formulated in previous sections, was coded in the Fortran IV language for use on a high speed digital computer. The wear model per se was implemented in the subroutine WEARL. Several programs, outlined in Table 3, were used to conveniently index certain parameters and generate related plots, but the WEARL subroutine was central to each program. A representative program, WEAR3, along with a sample of its output, and a brief description of both, is presented in Appendix A. A listing of the WEARL subroutine and a brief explanation of its operation are presented in Appendix B.

Of the several inputs required by the various wear programs, the primary input, common to all of the programs, is a digitized profile of the surface of interest. Some of the programs, WEAR3 of Appendix A included, are designed to perform computations on several digitized profiles, providing profile-to-profile comparisons of modeled wear. These programs often provide computed characteristics of the distribution of the wear predicted for several profiles, i.e., mean and sample standard deviation.

The various programs, input profiles, and other specific inputs were manipulated in an interactive computing environment. The system employed was IBM Corporation's Conversational Monitoring System, CMS, which operates within IBM's Virtual Machine Facility/370.

The profiles were acquired through the use of a Talysurf Surface Analyzer, Model 4, which had been modified to provide an analog voltage output proportional to the profile height. The analog signal was then digitized into 1024 discrete values of ten-bit resolution each, with

Table 3. Wear Simulation Programs

Program Name	Description
WEAR12 (option 1)	output type - plot number of profiles input - 1 ordinate - wear volume abscissa - penetration depth plots indexed over - sliding distance
WEAR12 (option 2)	output type - plot number of profiles input - 1 ordinate - wear volume abscissa - sliding distance plots indexed over - penetration depth
WEAR3	output type - table (see Appendix A) number of profiles input - 1 to 90 inputs - BAR, slider length, slider width, specific gravity of polymer, elongation at break of polymer, pin correction.
WEAR45 (option 1)	output type - plot number of profiles input - 1 to 16 ordinate - wear volume abscissa - BAR plots indexed over - one plot per profile
WEAR45 (option 2)	output type - plot number of profiles input - 1 to 16 ordinate - wear volume abscissa - sliding distance plots indexed over - one plot per profile
WEAR45A	same as WEAR45 except instead of plotting for each profile, the 95% confidence bands are plotted. (This was used to generate Fig. 30.)
WEAR6	output type - histogram number of profiles input - 1 ordinate - wear volume modeled at each wear site abscissa - location of wear site in profile indexed over - BAR
WEAR7	output type - histogram number of profiles input - 1 ordinate - wear volume modeled at each wear site abscissa - location of wear site in profile indexed over - sliding distance

a Zonic Technical Laboratories DMS/5003. The sample rate was chosen to provide a total profile length of approximately 0.6 mm. This was on the order of the diameter of the polymer pins used in wear tests, typically 0.55 mm. The digitized data were then transferred to CMS via a telephone line communications link, each transfer requiring about thirty seconds to complete. The entire profile acquisition system is shown schematically in Fig. 28. The on-line CMS storage capability, typically about fifty profiles, was augmented with off-line magnetic tape storage, permitting the efficient storage of several thousand profiles for later retrieval.

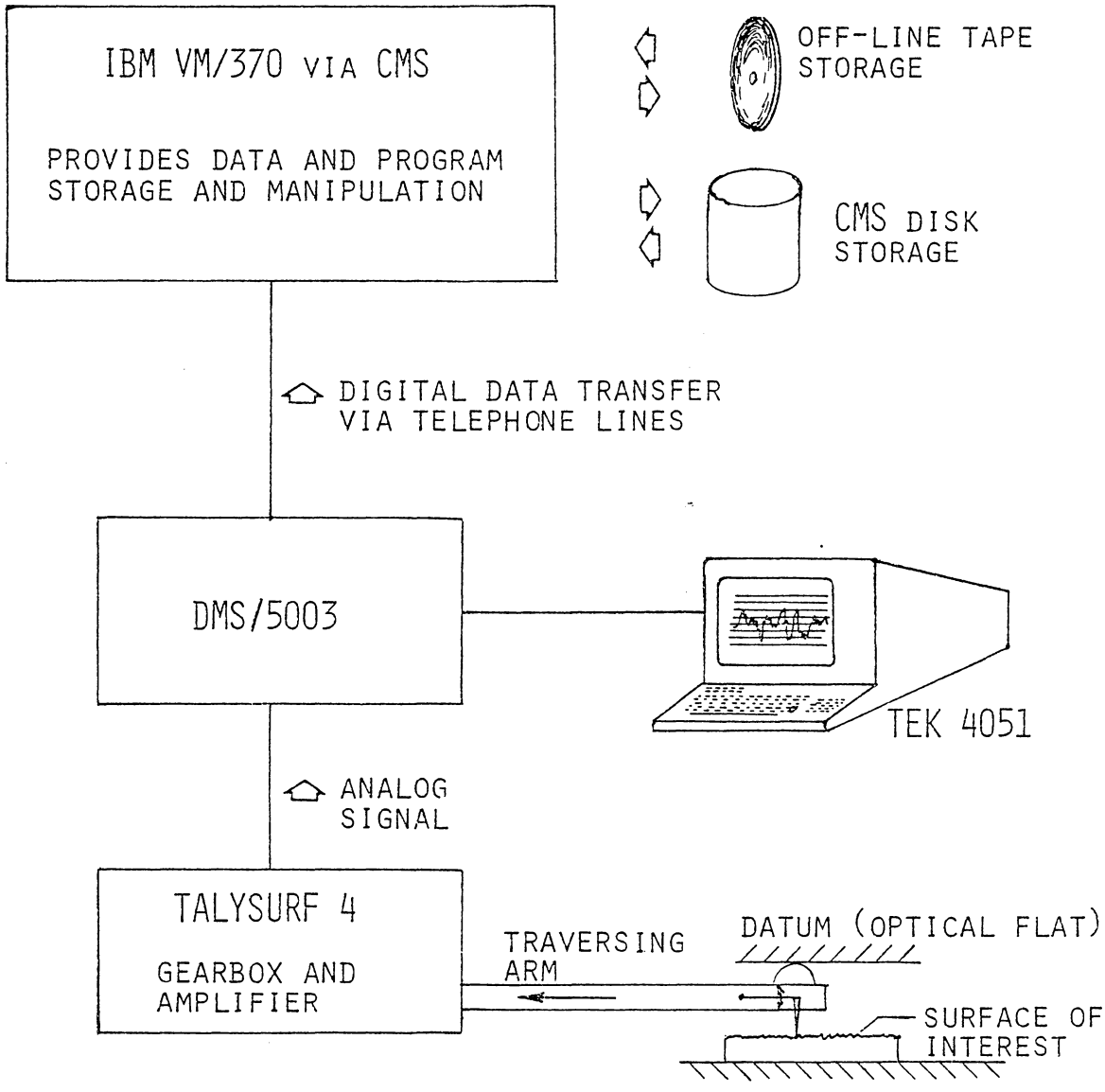

Figure 28. Data acquisition and manipulation system.

4. APPLICATION OF WEAR MODEL

In the wear model the polymer pin is assumed to have a rectangular cross section. Additionally it was assumed that the polymer was traversed in a direction normal to the lay of a ground surface. Unfortunately the wear data used to verify this model, which are presented in a later section, were not taken under the above mentioned assumed conditions. It was decided that the predicted wear should be modified by appropriate factors to render it in a form suitable for comparison with the available wear data. The next two sections discuss the development of these appropriate factors.

4.1. Lay of Counterface

This section contains a discussion of the development of the "lay correction" factor. This development is preceded by a description of the wear experiments carried out by Smyth [27]. In these experiments a unidirectionally ground steel disk was rotated while in contact with a polymer pin, much like a phonograph and needle. The radial position of the polymer pin on the steel disk was continuously varied during a given experiment so the pin would always encounter previously untouched metal surface assuring single pass conditions. The combined circular disk motion and radial pin motion created a spiral wear track, the average radius of which is taken as R . An experiment typically involved five disk revolutions. The mass of the polymer transferred to the steel as wear debris was then determined with a radiotracer technique [24]. The sliding distance was taken to be the average circumference of the spiral, $2 \cdot \pi \cdot R$, multiplied by the number of disk revolutions. The experimental results were then reported in units of mass transferred per unit sliding distance.

As developed, the present wear model incorporates the assumption that the polymer always moves normal to the grinding lay. However, in the experiments described, the polymer was sliding sometimes normal to, sometimes parallel to, and sometimes in a direction diagonal to the grinding lay, as shown in Fig. 29.

It was assumed that only sliding normal to the lay results in abrasive polymer wear. In the case of mixed normal and parallel sliding only the component normal to the lay was assumed to contribute to the wear of the polymer. In traversing a circular path of radius R, the

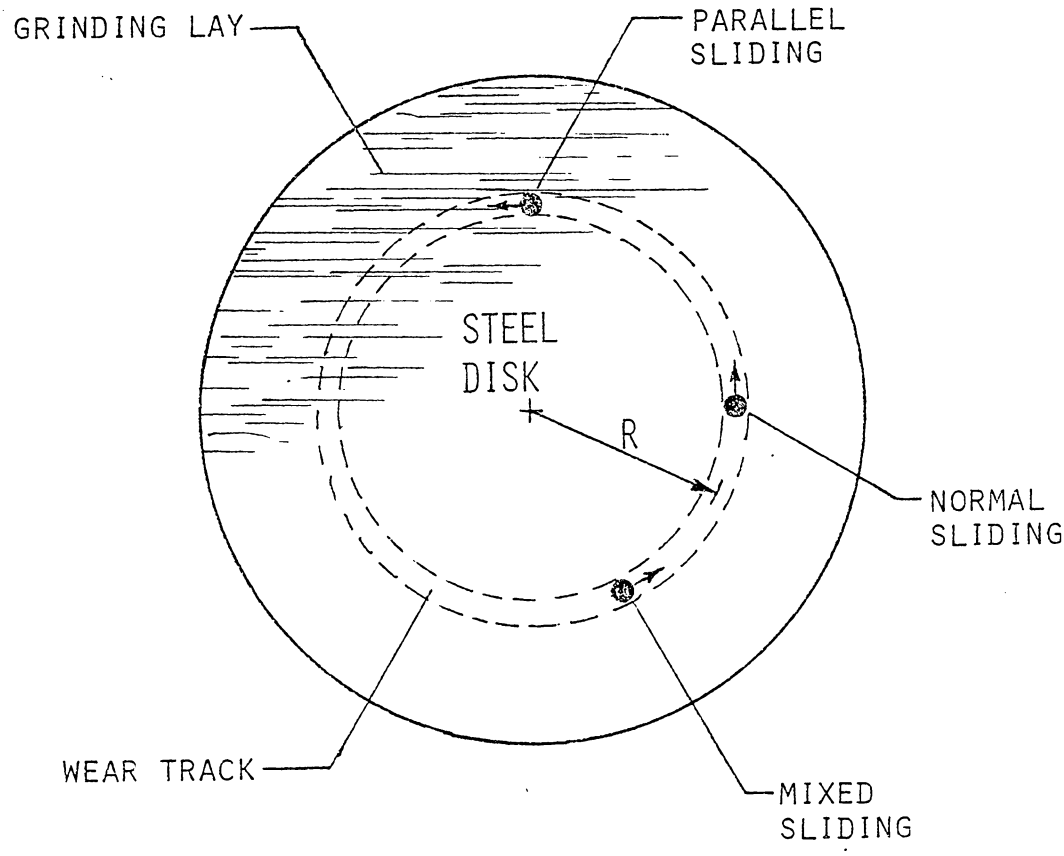

Figure 29. Wear track on unidirectionally ground disk.

polymer pin travels a distance of $2\pi R$. However, the total distance traveled by the polymer in a direction normal to the lay is two diameters, $2(2R) = 4R$. For one complete disk revolution, the ratio of the normal distance traveled to the actual distance traveled is $4R/2\pi R = 2/\pi$. Therefore, the modeled wear based on the actual distance traveled must be multiplied by a lay correction of $2/\pi$ to render it in a form comparable to the reported data.

4.2. Pin Geometry

This section contains a discussion of the development of the "pin correction" factor. The need for this correction arises from the fact that in the wear model the polymer pin is assumed to have a rectangular cross section, while the pins used in Smyth's experiments were circular in cross section. The model input most dependent on the geometry of the pin is the "slider length". In this model the slider length is defined as a distance equal to the length of the polymer pin in the direction of sliding. It is this slider length which, when combined with the wedge length and the factor G, determines the amount of wear debris collected at a given wear site. Hence, under single pass conditions, the slider length, D_s, is a dimension equal to the length of the modeled rectangular pin in the direction of sliding, as shown in Fig. 2. If two passes are made over the same region, the slider length is taken to be twice the slider length determined for single pass conditions.

Figure 30 serves to illustrate the effect of slider length on simulated wear. Each of the two bands shown represents a 95% confidence interval for the mean wear predicted for sixteen different profiles taken from the surfaces used in Smyth's experiments. There were four disks used for each roughness; and four profiles were taken from each disk. The asymptotic behavior of the predicted wear is attributed to the successive filling up of some of the void regions modeled. When a void is full, its respective cutting asperity no longer contributes to the wear of the polymer. When the slider length is extended to large values, all the voids eventually fill. This condition signals the termination of the transient stage of abrasive polymer wear.

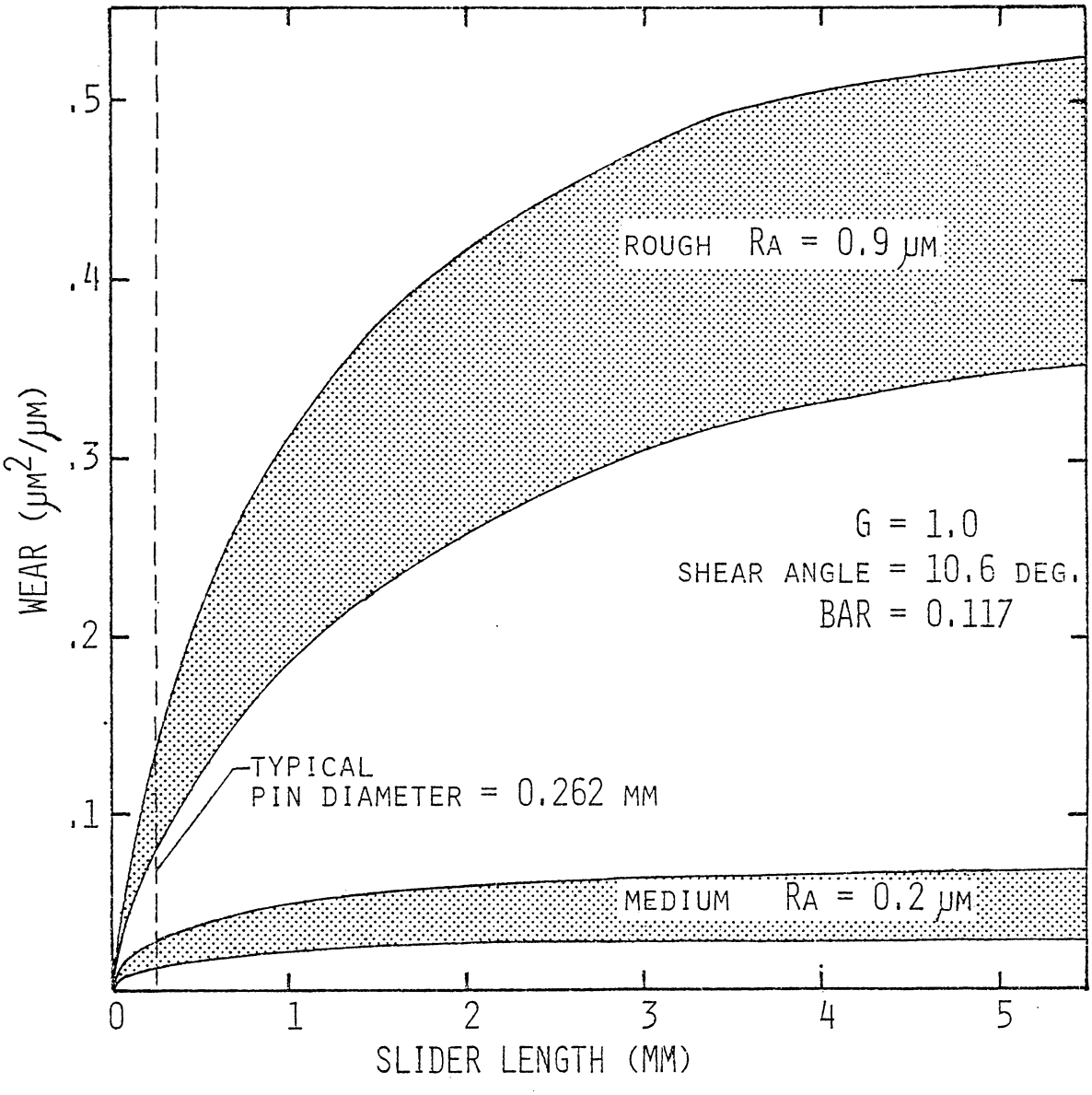

Figure 30. Modeled wear vs slider length for Smyth's [27] medium and rough surfaces. Bands represent the 95% confidence interval for the mean, each based on sixteen profiles.

It was decided that Smyth's circular pins would be modeled as rectangular pins of the same width, but whose length in the sliding direction is less than the pin diameter by a factor which yields the same apparent area as the circular pin, as shown in Fig. 31. The appropriate factor is readily found to be $\pi/4$.

There are two methods of incorporating this pin correction factor in the wear model. The diameter of the pin may be multiplied by the pin correction factor prior to inputting this dimension into the model as the slider length. Alternatively one may enter the actual pin diameter as the slider length. In this case the resulting modeled wear is then multiplied by the pin correction factor.

If a full pin diameter is entered as the slider length and the model calculates that none of the voids are full, the two methods of correcting for pin geometry are equivalent and predict identical values of wear. If a full pin diameter is entered as the slider length and the model calculates that some or all of the voids are full, the first method of correction will result in a wear overprediction, while the second method will result in a wear underprediction. The difference in the wear predicted by the two correction methods seldom exceeded ten percent for any of the predicted wear reported in the next section. It is interesting to note that when the second method is used, the pin correction factor is applied in a manner identical to the lay correction of the previous section, forming a combined factor of $(2/\pi)(\pi/4) = 0.5$.

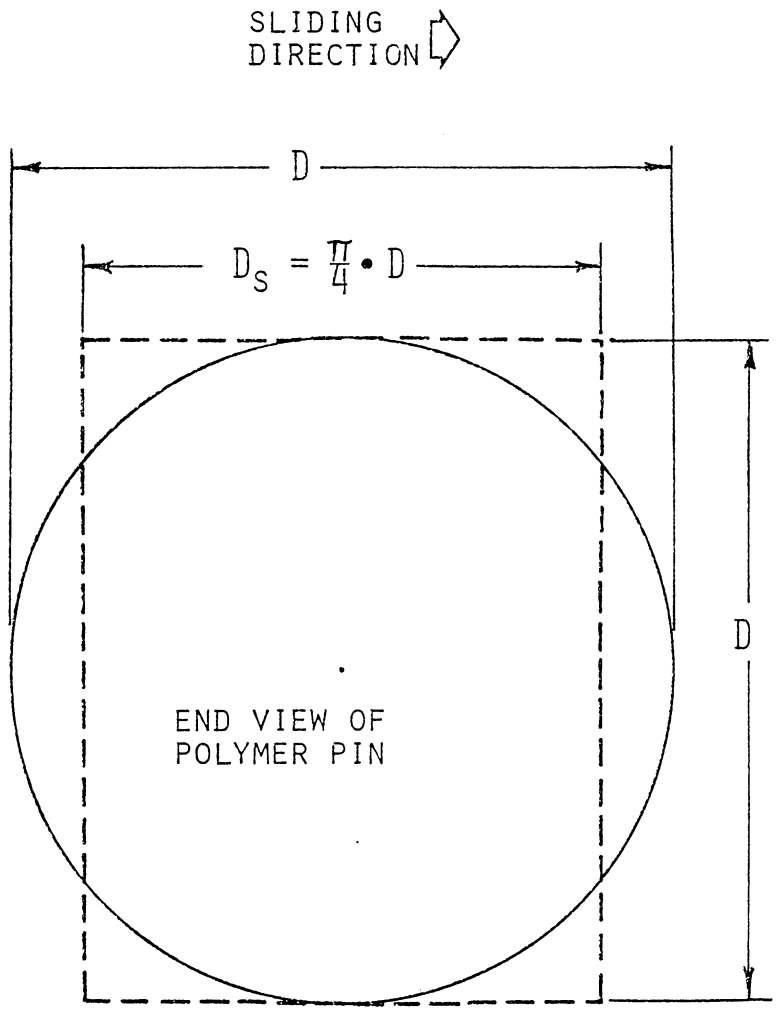

Figure 31. Development of Pin Correction Factor to model a circular polymer pin as a rectangle of the same area.

4.3. Mathematical Formulation of Wear Model

At this point all of the constituent parts of the wear model have been developed individually. This section contains the mathematical formulation of the model.

For the i^{th} asperity the wear volume, V_i, cannot exceed the void volume, V_{m_i}, where

$$V_{m_i} = D \cdot VA_i \quad . \tag{14}$$

Wear volume less than V_{m_i} is given by

$$V_{u_i} = \left[\frac{D_s}{G \cdot WL_i} \right] (D \cdot WA_i) \quad , \tag{15}$$

where the first term is the number of wedges worn at asperity i; and the second term is the volume of each wedge. The total wear volume, V, is given as

$$V = \frac{d}{L} \sum_{i=1}^{N} V_i \quad , \tag{16}$$

where the quantity d/L is the ratio of the total sliding distance to the sampled portion of that distance. Equation 16, when corrected for unidirectional lay, becomes

$$V = \frac{2}{\pi} \frac{d}{L} \sum_{i=1}^{N} V_i \quad . \tag{17}$$

To correct for a circular pin using method 1, the slider length is given by

$$D_s = \frac{\pi}{4} D \quad . \tag{18}$$

Substituting Eq. 18 into Eq. 15 yields

$$V_{u_i} = \left[\frac{\frac{\pi}{4} D}{G \cdot WL_i}\right] (D \cdot WA_i) = \frac{\pi}{4} \frac{D^2 \cdot WA_i}{G \cdot WL_i} \quad . \quad (19)$$

To correct for a circular pin using method 2, the slider length is taken to be the pin diameter, $D_s = D$. Thus, Eq. 15 becomes

$$V_{u_i} = \left[\frac{D}{G \cdot WL_i}\right] (D \cdot WA_i) = \frac{D^2 \cdot WA_i}{G \cdot WL_i} \quad , \quad (20)$$

and the worn volume is given by

$$V = \frac{\pi}{4} \frac{2}{\pi} \frac{d}{L} \sum_{i=1}^{N} V_i \quad . \quad (21)$$

If no filling occurs, then $V_i = V_{u_i}$ always. Thus, either lay correction will result in the following equation for volume of wear.

$$V = \frac{\pi}{4} \frac{2}{\pi} \frac{d}{L} \frac{D^2}{G} \sum_{i=1}^{N} \frac{WA_i}{WL_i}$$

$$= 0.5 \frac{d}{L} \frac{D^2}{G} \sum_{i=1}^{N} \frac{WA_i}{WL_i} \quad . \quad (22)$$

4.4. Model Verification

The results of Smyth's experiments [27] were used to verify the model. In these experiments Smyth conducted wear tests on surfaces of three roughnesses: R_a = 0.05 μm termed smooth, R_a = 0.2 μm termed medium, and R_a = 0.9 μm termed rough. Four disks were ground to each roughness. On each of the twelve disks, three polymers were tested: PVC, PCTFE, and LDPE. Of these polymers only PVC and PCTFE were tested below their T_g's. Therefore, only the results of the PVC and PCTFE wear tests were used for this model verification.

Smyth's wear data were measured and reported in units of mass transferred per unit sliding distance, specifically, μg/m. For convenience, these data are reported in this section in units of volume per unit sliding distance, mm^3/km. These units of mm^3/km were also used for all wear predictions. The specific gravities of PVC and PCTFE were taken to be 1.35 and 2.2, respectively.

Table 4 shows Smyth's wear data and the wear predicted by the model for the same conditions. The predictions, shown in parentheses, were evaluated and tabulated for both pin correction methods. It should be noted that a value of G = 1.0 was used to generate the first two columns of wear predictions. The third column of wear predictions, where G = 4.8, represents a further sophistication of the model.

As mentioned in a previous section, it was felt that the factor G should be a function of the elongation at break of the polymer being simulated. As can be seen in Table 4, the model overpredicts the wear of PVC by a factor of roughly two, and it overpredicts the wear of PCTFE by a factor of roughly ten. Considered together, the error in

Table 4. Experimental and Predicted Wear Data

Disk	Wear Rate, mm^3/km — Polymer: PVC measured	PVC predicted $\phi = 10.6°$ $G = 1.0$	PCTFE measured	PCTFE predicted $\phi = 12.8°$ $G = 1.0$	PCTFE predicted $\phi = 12.8°$ $G = 4.8$
Smooth R_a = .05 μm					
A11	0.19 †	(0.04/ 0.03)*	0.22	(- / -)**	(- / -)
B11	0.25	(0.00/ 0.00)	0.05	(- / -)	(- / -)
A12	0.00	(- / -)	0.00	(- / -)	(- / -)
B12	0.00	(- / -)	0.15	(- / -)	(- / -)
Medium R_a = .2 μm					
A21	2.66 ††	(5.52/ 5.07)	1.57	(12.11/11.26)	(4.64/ 4.20)
B21	1.84	(3.95/ 3.51)	1.75	(8.19/ 7.18)	(3.54/ 3.13)
A22	2.95	(8.35/ 7.48)	0.93	(20.37/16.85)	(7.31/ 7.22)
B22	1.82	(3.84/ 3.50)	1.41	(9.18/ 8.04)	(3.47/ 3.38)
Rough R_a = .9 μm					
A31	17.56 †††	(28.17/26.59)	7.95	(76.82/69.02)	(25.14/23.90)
B31	13.11	(26.08/24.11)	8.95	(80.25/74.68)	(28.04/25.83)
A32	18.00	(28.59/26.87)	5.95	(88.28/78.59)	(28.99/26.52)
B32	13.63	(20.64/18.95)	9.50	(55.35/49.94)	(19.96/18.69)

† For this roughness, the accuracy of the data is ±0.01.

* (x.xx/ x.xx) Left hand side is using pin correction method 1. Right hand side is using pin correction method 2.

** " - " indicates that no wear sites were detected for given conditions.

†† For this roughness, the accuracy of the data is ±0.04.

††† For this roughness, the accuracy of the data is ±0.08.

the PCTFE wear predictions is roughly five times the error in the PVC wear predictions. It is here one notes that the ratio of the elongation at break for PCTFE to that of PVC is 1.25/0.263 = 4.8 (ε values from [24, p. 30]). Stated differently, PCTFE stretches about 4.8 times further than does PVC before it breaks. Since PVC was the closer of the two in predicted values of wear, it was decided that the factor G for PVC should remain equal to 1.0 ; and the value of G for PCTFE should be set equal to 4.8 . The effect of this value of G for PCTFE is shown in the third column of wear predictions in Table 4.

If no filling occurs in the wear model, the predicted wear would vary in an inverse proportion to G (ref. Eq. 22). The fact that increasing G by a multiple of 4.8 decreased the predicted wear by a lesser factor is an indication that some filling occurred in the wear simulation. The filling was monitored for all of the wear simulation results shown in Table 4, and ranged from 0 to 76% of the available void regions.

5. DISCUSSION

The wear simulation results shown in Table 4 indicate that the model does, to an acceptable extent, predict abrasive polymer wear. The accuracy of this model is better appreciated in light of wear data presented in the literature. Researchers report wear rates which often vary by several orders of magnitude in response to seemingly minor changes in one or more of the system and environmental test parameters. Researchers, in attempting to duplicate tests of others, often find it difficult to corroborate findings of others. Finally, replications of wear experiments typically result in data variances so great that researchers are (or should be) reluctant to place undue significance on their results.

As formulated, the modeling of abrasive polymer wear occurs in three distinct phases: penetration of the polymer into the ground surface, the development of a wear particle geometry, and the accumulation of wear particles. Each of these phases contains hypotheses and assumptions which warrant additional mention.

The polymer flow pressure, p_m, is central to the penetration phase of the model. It was taken to be three times the yield stress in tension. No consideration was given to strain rate dependencies, strain hardening, additional interfacial pressure components contributed by friction and tangential cutting forces, or distortion of the contact area due to tangential forces, viscoelastic deformations, or material removal. The effect of possible load support by polymer wear debris trapped in filled void regions was also neglected. Only the effect of

asperity slope was examined. Although slope was shown to be an important factor in the determination of the flow pressure, incorporation of the relationship in the model was found to be intractable.

The polymer shear angle, ϕ, is central to the section of the model which determines the geometry of wear particles. This shear angle was based on Warren's work concerning the average angle of polymer deposits. Modeling a complex failure zone in the polymer as a singular angle is doubtless an oversimplification of the event leading to the production of a wear particle. It does, however, yield a model in which the wear predicted at an asperity is functionally related to the slope of the asperity. Indeed it is this parameter which determines whether or not a penetrating asperity will cut at all.

The factor G is central to the section of the model which determines the rate of particle formation at each asperity. It was felt that this factor should be a function of the elongation at break of the polymer. However, for lack of an acceptable theory, this factor was initially assumed to be unity. Later, having compared predicted wear values to experimental values, it was decided that the value of G for a polymer would be taken to be the ratio of the elongation at break for the polymer to the elongation at break for PVC. This effectively establishes G = 1.0 for PVC.

It should be noted that the decision to obtain values for G by dividing by the elongation at break for this particular polymer, PVC, was based solely on the closer agreement between predicted and experimental wear values for PVC. Dividing by yet another value would have yielded wear predictions closer to experimental values, but would have

had no clear theoretical basis. No hypothesis is advanced for determining correct values for G other than they should be greater than 0.5. Additionally, care should be taken to assure that the values for the elongation at break of the polymers modeled are all measured in the same fashion.

The predicted wear values of Table 4 exhibit an interesting trend. The predicted wear for PVC and for PCTFE with G = 4.8 are almost equal. Although the operating BARs were similar in all cases (BAR = 0.11), these predictions were based on different shear angles, values of G, and test pin diameters. The average pin diameters were 0.266 mm for PVC, and 0.565 mm for PCTFE. It is clear when comparing the predicted wear for PVC and PCTFE with G = 1.0, that differences in the pin diameter and shear angle result in large variations in predicted wear. When G is then set equal to 4.8 for PCTFE, it approximately compensates for the differences in shear angles and pin diameters used. This is felt to be due only to a fortuitous choice of test polymers and pin diameters; and it is noted that wear data for the two polymers are similar also. It is not anticipated that other polymers will demonstrate this phenomenon.

6. CONCLUSIONS

While certain points in the model are less than totally substantiated, the general philosophy of the modeling technique used is both unique and useful. In an abrasive wear process, each asperity presents a unique potential wear site. The model, in turn, simulates the wear process on a site-by-site basis.

This work represents two distinct contributions. First, the computer environment and the data handling and storage techniques developed comprise a method of testing any well stated wear theory. Little additional effort would be required to evaluate alternative models of surface interpenetration and wear particle formation.

Second, a model of the abrasive polymer wear process was advanced and evaluated in light of a restricted quantity of experimental data. Although it is inexact in some respects, it is felt that this model demonstrates all the salient features of the abrasive polymer wear phenomenon.

7. RECOMMENDATIONS

Several aspects of the polymer wear model require further investigation. The following is a list of recommendations beginning with those the author deems most important.

1) Additional data should be taken using PVC, PCTFE, and other polymers at temperatures below their T_g's. Different BARs should be used for these tests. Nylon 6-6 would be a suitable candidate polymer for further testing since its shear angle was determined by Warren. Polymers other than PVC, PCTFE, and Nylon 6-6 would require additional observation to determine their shear angles.

2) The penetration of the polymer into the counterface is currently computed using a polymer flow pressure and the BAR curve of the counterface. An experimental program should be developed to confirm or improve this method of determining the penetration depth. Deterministic surfaces similar to the one discussed earlier in this dissertation might be constructed of glass or a similar hard, transparent material, allowing the researcher to observe the penetration from the reverse side of the material. These observations, likely employing an optical microscope, would provide a means of determining the effect of factors such as normal load, tangential load, asperity angle, and others, on the penetration of the polymer into the counterface.

3) The extension of this model to include steady state wear conditions, reciprocating sliding conditions, high sliding speeds, and polymers above their T_g's, will require considerable additional investigation. The philosophy of this model should, however, provide a useful environment in which to develop models for more complex wear conditions.

8. REFERENCES

1. Dourlet, E. F., "Selecting Plastics," Machine Design, Plastics/ Elastomers Reference Issue, Vol. 43, No. 4, 11 Feb., 1971, pp. 1-4.

2. Steijn, R. P., "Friction and Wear of Plastics," Metals Engineering Quarterly, Vol. 7, No. 2, American Society for Metals, May 1967, pp. 9-21.

3. Briscoe, B. J., C. M. Pooley, and D. Tabor, "Friction and Transfer of Some Polymers in Unlubricated Sliding," Advances in Polymer Friction and Wear, Vol. 5A, L. H. Lee, Ed., Plenum Press, New York, 1974, p. 191.

4. Lancaster, J. K., "Abrasive Wear of Polymers," Wear, Vol. 14, 1969, pp. 223-239.

5. Lancaster, J. K., "Basic Mechanisms of Friction and Wear of Polymers," Plastics and Polymers, Vol. 41, 1973, pp. 297-306.

6. Lee, L. H., "Effect of Surface Energetics on Polymer Friction and Wear," Advances in Polymer Friction and Wear, Vol. 5A, L. H. Lee, Ed., Plenum Press, New York, 1974, p. 31.

7. Jain, V. K., and S. Bahadur, "Development of a Wear Equation for Polymer-Metal Sliding in Terms of Fatigue and Topography of Sliding Surfaces," Wear of Materials 1979, K. C. Ludema, W. A. Glaeser, and S. K. Rhee, Ed., ASME, New York, pp. 556-562.

8. Godet, M., D. Play, and D. Berthe, "An Attempt to Provide a Unified Treatment of Tribology Through Load Carrying Capacity, Transport, and Continuum Mechanics," ASME Paper No. 79-LUB-18.

9. Archard, J. F., and W. Hirst, "The Wear of Metals Under Unlubricated Conditions," Proc. Royal Soc. London, Series A, Vol. 236, 1956, p. 397-410.

10. Bowden, F. P., and D. Tabor, The Friction and Lubrication of Solids, Part I, Oxford University Press, Ely House, London, 1950, pp. 10-14.

11. Rabinowicz, E., Friction and Wear of Materials, John Wiley and Sons, New York, 1965.

12. Halliday, J. S., "Surface Examination by Reflection Electron Microscopy," Proceedings of the Institute of Mechanical Engineers, Vol. 169, London, 1955, pp. 777-781.

REFERENCES (cont'd)

13. Greenwood, J. A., and J. B. P. Williamson, "Contact of Nominally Flat Surfaces," Proc. Royal Soc. London, Series A, Vol. 295, 1966, pp. 300-319.

14. Ernst, H., and M. E. Merchant, "Chip Formation, Friction and Finish," Surface Treatment of Metals, American Society for Metals, Cleveland, Ohio, 1941, pp. 299-378.

15. Kobayashi, S., and E. G. Thomsen, "Metal Cutting Analysis -1, Re-Evaluation and New Method of Presentation of Theories," Trans. ASME, Series B, Journal of Engineering for Industry, Vol. 84, No. 1, Feb. 1962, pp. 63-70.

16. Merchant, M. E., "Mechanics of the Metal Cutting Process. II. Plasticity Conditions in Orthogonal Cutting," Journal of Applied Physics, Vol. 16, June 1945, pp. 318-324.

17. Rao, U. M., J. D. Cumming, and E. G. Thomsen, "Some Observations on the Mechanics of Orthogonal Cutting of Delrin and Zytel Plastics," Trans. ASME, Series B, Journal of Engineering for Industry, Vol. 86, No. 2, May 1964, pp. 117-121.

18. Bowden, F. P., and D. Tabor, The Friction and Lubrication of Solids, Part II, Oxford: Clarendon Press, 1964, p. 333.

19. Hill, R., E. H. Lee, and S. J. Tupper, "The Theory of Wedge Indentation of Ductile Materials," Proc. Royal Soc. London, Series A, Vol. 188, 1947, pp. 273-291.

20. Tabor, D., The Hardness of Metals, Oxford: Clarendon Press, 1951.

21. Samuels, L. E., and T. O. Mulhearn, "An Experimental Investigation of the Deformed Zone Associated with Indentation Hardness Impressions," J. Mech. Phys. Solids, Vol. 5, 1957, pp. 125-134.

22. Johnson, K. L., "The Correlation of Indentation Experiments," J. Mech. Phys. Solids, Vol. 18, 1970, pp. 115-126.

23. Hirst, W., and G. J. W. Howse, "The Indentation of Materials by Wedges," Proc. Royal Soc. London, Series A, Vol. 311, 1969, pp. 429-444.

24. Warren, J. H., The Prediction of Polymer Wear Using Polymer Mechanical Properties and Surface Characterization Parameters, Doctoral Dissertation, Virginia Polytechnic Institute and State University, Blacksburg, Virginia, August 1976.

REFERENCES (cont'd)

25. Ratner, S. B., I. I. Farberova, O. V. Radyukevich, and E. G. Lur'e, "Connection Between the Wear Resistance of Plastics and Other Mechanical Properties," Abrasion of Rubber, D. I. James, Ed., Maclaren, London, 1967, pp. 145-155. (Translated from Soviet Plastics, n. 7, 1964)

26. Lancaster, J. K., "Relationships Between the Wear of Polymers and Their Mechanical Properties," Proc. Institution of Mechanical Engineers, Series 3P, Vol. 183, January 1969, pp. 98-106.

27. Smyth, K. A., A Study of Polymer Wear by the Abrasive and Adhesive Mechanisms, Master's Thesis, Virginia Polytechnic Institute and State University, Blacksburg, Virginia, August 1979.

9. APPENDIX A: DESCRIPTION AND LISTING OF WEAR3

DESCRIPTION AND LISTING OF WEAR3

This appendix is made up of four parts: a) a description of the important features of the Fortran program WEAR3, b) a block diagram of WEAR3, c) a listing of WEAR3, and d) a sample output generated by WEAR3.

WEAR3 simulates polymer wear on any number of input profiles, each in turn, and determines the appropriate averages for the group of profiles. The simulation is carried out twice for each profile, once "forward", and once "backward". This is equivalent to conducting wear tests in opposite directions on the same surface.

The program contains comment lines for clarity. The first three pages of the program listing contain startup information such as the number of profiles to be inputted, and the data necessary for the simulation such as operating BAR, sliding distance, shear angle, and the factor G. The major loop of the program ("DO 1000 PROF=1,NPROF") begins on the fourth page. This loop, executed once for each profile, starts with three subroutines: READ1, NORM1, and RANK1. A listing of each of these subroutines is found at the end of the WEAR3 listing.

The READ1 subroutine is a sophisticated routine which disregards lines not in a profile format and distinguishes which of two common formats was used to store the data. It then reads the profile data into the Y array.

The NORM1 subroutine removes the slope and/or the average of the profile. The slope removal is based on a least squares fit of a straight

line through the data. Whether or not the profiles are "normalized" is a user option and is recorded in the output.

The third subroutine, RANK1, uses an efficient method to rank the Z array, an array initially identical to the Y array. Once ranked, largest value to smallest value, the height corresponding to the BAR is equal to that value of Z found at the fraction of the Z array equal to the BAR. The penetration depth is the difference between this height value, and the highest point in the profile, now contained in the array position Z(1). If the BAR used does not provide an integer index for the Z array, a linear interpolation is utilized between the bracketing Z values to obtain the height. The penetration depth determined for each profile is recorded in the output in the column headed by "penet".

At this point in the program a few surface statistics are computed to serve as a profile signature and to provide background information about the surface. The R_a roughness and the skewness of the profile are calculated and recorded in the program output.

After the statistics of the profile are calculated, an additional loop is entered ("DO 25 DIRECT=1,2") to simulate the wear forward and backward. The second time through the loop the input Y array is reversed end for end and the simulation then proceeds as in the first time through.

At this point the subroutine WEARL is invoked. Five arrays and an integer are returned from WEARL. These arrays are named WL, WA, VA, ICAP, and LOC. The integer value returned, IPAIR, contains the number of wear sites detected by WEARL. WL(i) contains the modeled wedge length at site i, WA(i), the corresponding wedge area, VA(i), the

corresponding void area. ICAP(i), the integral capacity of void i (ICAP(i) = VA(i)/WA(i) + 1), and LOC(i) contains the index of the point in the profile array Y where the wear site i was modeled to begin. Given these returned values, WEAR3 then computes the sum of the wedges at each site for the given sliding distance and factor G.

Several features of the WEAR3 output, presented at the end of this appendix, have already been discussed. However, a few others deserve mention. The date given in the output (in this case 05-01-80) represents the date of the simulation. The data for this feature result from the CALL DATE in WEAR3. The next four lines of output contain the simulation parameters. The output line beginning with "1) B32A..." will be examined as an example. The B32A is a profile identifier. As indicated, 12 wear sites were detected when simulating wear in a forward direction, and 11 were detected in the reverse direction. As listed the wear detected in the two directions varied from 14.7 mm^3/km forward, to 23.0 mm^3/km backward. The 14.7 mm^3/km represents 10.% of the total available void volume in the forward direction; and the 23.0 mm^3/km represents 13.% of the total available void volume in the backward direction. Filling of some voids may or may not have occurred.

Below the second line of dashes several averages are recorded. While most of them are clear, a few require explanation. The quantity 6.113 represents the sample standard deviation of the population of eight simulated wear values. The 32.7 quantity is the percentage of 18.687 represented by 6.113 . This 32.7 quantity provides a means of evaluating the scatter in the simulated wear values. Finally, the figure of 151.3 is the average number of lumps, or wedges, counted

as worn at each wear site, averaged over all wear sites and all profiles, forward and backward.

Block Diagram of Program WEAR3

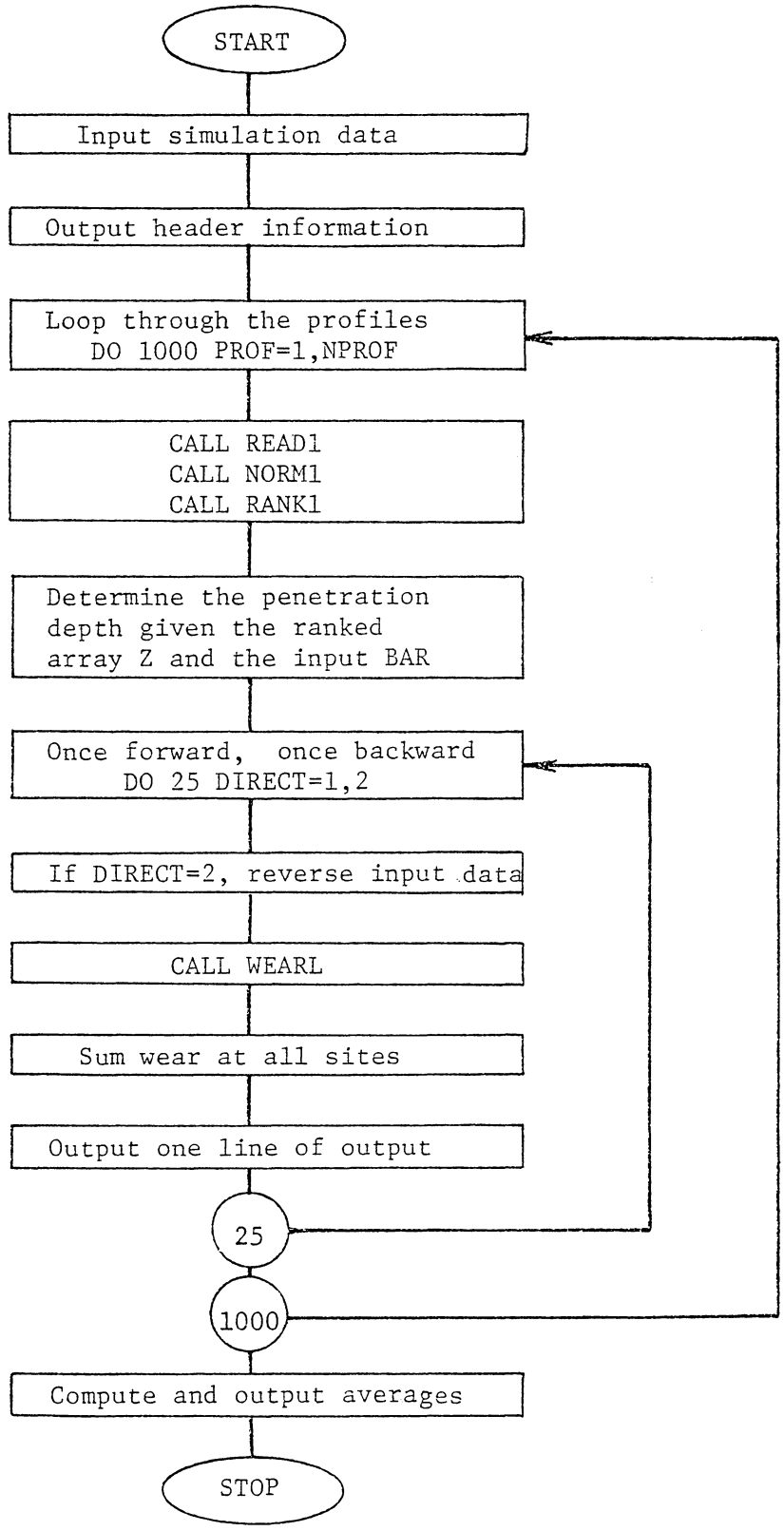

```
C ****************************************************************
C *                                                              *
C *    Polymer Wear Simulation Program WEAR3                     *
C *    Written Fall 1979, by John H. Herold                      *
C *                                                              *
C ****************************************************************
C
      INTEGER TERMIN,OUTFIL,FILE,UNIT,PROF,FILTYP,DIRECT
      INTEGER PAIR,PAIRS,PAIRAV
      REAL LENGTH,LMPSUM
      COMMON/A/UNIT,FILTYP,NP,DX,Y(1500),COMENT(40),DATT(3),
     $LABEL(18)
      COMMON/D/TERMIN,WL(200),WA(200),VA(200),ICAP(200),
     $TANANG,LOC(200)
      DIMENSION FN(10,2),FT(10,2),FM(10,2),PERFL(2),AVPER(2)
      DIMENSION WEAR(2),WEARAV(3),Z(1500),PAIRS(2),PAIRAV(2)
      DATA WEARAV/3*0./,PAIRAV/2*0/,AVPER/2*0./
      TERMIN=1
      OUTFIL=2
      CALL DATE(IM,ID,IY)
      READ(TERMIN,*,END=2)NPROF,NFILE,NORM,MASORV
      DO 1 FILE=1,NFILE
      READ(TERMIN,100,END=2)FN(FILE,1),FN(FILE,2)
      READ(TERMIN,100,END=2)FT(FILE,1),FT(FILE,2)
    1 READ(TERMIN,100,END=2)FM(FILE,1),FM(FILE,2)
  100 FORMAT(2A4)
      GOTO 4
    2 REWIND TERMIN
      WRITE(TERMIN,110)
  110 FORMAT(//,'An error has apparently occurred in the ',
     $'internal exchange of',/'control parameters from ',
```

```
     $'WEAR3 EXEC to WEAR3 FORTRAN.'/'This is necessarily ',
     $'a fatal error.')
      STOP
    3 REWIND TERMIN
    4 WRITE(TERMIN,120)
  120 FORMAT(/,'Please enter the BAR to be used ',
     $'for this test.')
      READ(TERMIN,*,END=3)BEARAT
      IF(BEARAT.GT.1..OR.BEARAT.LT.0.)GOTO 4
      GOTO 6
    5 REWIND TERMIN
    6 WRITE(TERMIN,130)
  130 FORMAT(/,'Please enter the sliding distance ',
     $'(pin diameter (mm)).')
      READ(TERMIN,*,END=5)SLIDE
      TRAVEL=SLIDE*1000.
C     This converts the mm sliding distance into microns.
      IF(MASORV.EQ.3)GOTO 9
      WRITE(TERMIN,140)SLIDE
  140 FORMAT('Please enter the slider width. ',
     $'- default is ',F5.3,' mm.')
      READ(TERMIN,*,END=7)WIDTH
      GOTO 9
    7 REWIND TERMIN
      WIDTH=SLIDE
      GOTO 9
    8 REWIND TERMIN
    9 WRITE(TERMIN,150)
  150 FORMAT('Please specify the shear angle desired.',
     $'  Suggested values are:',/,'10.6 for PVC, 12.8 for ',
     $'PCTFE, and 18.9 for Nylon 6-6.')
      READ(TERMIN,*,END=8)ANGLE
      IF(ANGLE.LE.0..OR.ANGLE.GE.90.)GOTO 9
      ANGRAD=ANGLE*3.14159265 4/180.
      TANANG=TAN(ANGRAD)
      GOTO 11
   10 REWIND TERMIN
   11 WRITE(TERMIN,160)
  160 FORMAT(/'Please specify the elongation ratio, G, ',
     $'desired.  Suggested values are:',/,'1.0 for PVC, ',
     $'4.8 for PCTFE, and 9.1 for Nylon 6-6.')
      READ(TERMIN,*,END=10)G
      IF(G.LT.0.5)GOTO 11
      CONST=(G-0.5)/G
      IF(MASORV.EQ.2.OR.MASORV.EQ.3)GOTO 15
      GOTO 13
   12 REWIND TERMIN
   13 WRITE(TERMIN,170)
  170 FORMAT(/'Please specify the polymer''s specific ',
```

```
     $'gravity.  Suggested values are:',/,'1.35 for PVC, ',
     $'2.2 for PCTFE, and 1.1 for Nylon 6-6.')
      READ(TERMIN,*,END=12) SPGRAV
      GOTO 15
   14 REWIND TERMIN
   15 WRITE(TERMIN,180)
  180 FORMAT(/'Please specify the combined pin and lay co',
     $'rrection factor.',/,' The suggested value is 0.5 .')
      READ(TERMIN,*,END=14) PINLAY
      IF(MASORV.EQ.1) FACTOR=PINLAY*1000.*WIDTH*SPGRAV
      IF(MASORV.EQ.2) FACTOR=PINLAY*1000.*WIDTH
      IF(MASORV.EQ.3) FACTOR=PINLAY*1000.
      WRITE(OUTFIL,190) IM,ID,IY
  190 FORMAT(20X,'Output of program WEAR3   ',
     $A2,'-',A2,'-',A2,/)
      IF(NORM.EQ.1) WRITE(OUTFIL,201) BEARAT,SLIDE
      IF(NORM.EQ.2) WRITE(OUTFIL,202) BEARAT,SLIDE
  201 FORMAT(' BAR=',F6.4,',    Slider length (mm)=',
     $F6.4,',     Non-normalized')
  202 FORMAT(' BAR=',F6.4,',    Slider length (mm)=',
     $F6.4,',         Normalized')
      IF(MASORV.EQ.1) WRITE(OUTFIL,211) ANGLE,WIDTH,G,SPGRAV,
     $PINLAY
      IF(MASORV.EQ.2) WRITE(OUTFIL,212) ANGLE,WIDTH,G,PINLAY
      IF(MASORV.EQ.3) WRITE(OUTFIL,213) ANGLE,G,PINLAY
  211 FORMAT(' Shear angle (deg)=',F4.1,', Slider width ',
     $'(mm)=',F5.3,','/' Elongation ratio, G,=',F4.1,' , S',
     $'pecific gravity=',F6.3,' ,'/' The combined pin and ',
     $'lay correction=',F6.4,' .',//' CMS FILE ID',
     $'      STATISTICS',18X,'WEAR RATE ( ug/m )')
  212 FORMAT(' Shear angle (deg)=',F4.1,', Slider width ',
     $'(mm)=',F5.3,','/' Elongation ratio, G,=',F4.1,' .',
     $/' The combined pin and lay correction=',F6.4,' .',
     $//' CMS FILE ID      STATISTICS',18X,'WEAR VOLUME ',
     $'( cu.mm/km )')
  213 FORMAT(' Shear angle (deg)=',F4.1,' , Elongation ',
     $'ratio, G,=',F4.1,' ,'/' The combined pin and lay ',
     $'correction=',F6.4,' .',//' CMS FILE ID',
     $'      STATISTICS',18X,'WEAR THICHNESS ( nm )')
      WRITE(OUTFIL,220)
  220 FORMAT('    (FN)          ',
     $'Ra  skew   penet',8X,'Forward',9X,'Backward',/,
     $14X,'(um)',9X,'(um)   Pairs Wear %Full   Pairs ',
     $'Wear %Full',/,69('_'),/)
      RAAVE=0.
      SKEWAV=0.
      PENAVE=0.
      STDDEV=0.
      LMPSUM=0.
```

```
      DENOM=0.
      UNIT=10
      DO 1000 PROF=1,NPROF
      CALL READ1
      FILE=UNIT-9
      CALL NORM1(2,NORM)
      LENGTH=NP*DX
      DO 16 I=1,NP
   16 Z(I)=Y(I)
C
C     The array 'Z' will be put through the ranking process
C     to determine the penetration depths, then discarded.
C
      CALL RANK1(1,NP,Z)
C
C     Now we'll find the penetration depth for this profile.
C
      IF(BEARAT.EQ.0.)GOTO 17
      IF(BEARAT.EQ.1.)GOTO 18
      RN=BEARAT*NP
      NLO=RN
      NHI=NLO+1
      PENET=Z(1)-Z(NHI)+(NHI-RN)*(Z(NLO)-Z(NHI))
      GOTO 19
   17 PENET=0.
      GOTO 19
   18 PENET=Z(1)-Z(NP)
   19 PENAVE=PENAVE+PENET
C
C     Let's compute some stats; namely the Ra and the SKEW.
C
      THERA=0.
      THEMS=0.
      SKEW=0.
      DO 20 I=1,NP
      THERA=THERA+ABS(Y(I))
      THEMS=THEMS+Y(I)*Y(I)
   20 SKEW=SKEW+Y(I)**3
      THERA=THERA/NP
      RAAVE=RAAVE+THERA
      THEMS=THEMS/NP
      THERMS=SQRT(THEMS)
      SKEW=(SKEW/NP)/(THERMS**3)
      SKEWAV=SKEWAV+SKEW
C
C     Now let's compute the wears forward and backward.
C
      DO 25 DIRECT=1,2
      IF(DIRECT.EQ.2)GOTO 21
```

```
      GOTO 23
C     This part inverts the Y array if DIRECT=2.
   21 NOVER2=NP/2
      NPP=NP+1
      DO 22 I=1,NOVER2
      DUMMY=Y(NPP-I)
      Y(NPP-I)=Y(I)
   22 Y(I)=DUMMY
   23 IBEGIN=1
      HPOLY=Z(1)-PENET
C
C
      CALL WEARL(NP,IBEGIN,Y,HPOLY,DX,IPAIR)
C
C
      PAIRS(DIRECT)=IPAIR
      WEAR(DIRECT)=0.
      PERPL(DIRECT)=100.
      IF(IPAIR.EQ.0)GOTO 25
      W=0.
      TOTAL=0.
      DO 24 PAIR=1,IPAIR
      WEDGES=TRAVEL/(G*WL(PAIR))+CONST
      LUMPS=WEDGES
      IF(ICAP(PAIR).LT.LUMPS)LUMPS=ICAP(PAIR)
      LMPSUM=LMPSUM+LUMPS

      W=W+LUMPS*WA(PAIR)
   24 TOTAL=TOTAL+ICAP(PAIR)*WA(PAIR)
      WEAR(DIRECT)=W/LENGTH*FACTOR
      PERPL(DIRECT)=W/TOTAL*100.
      PAIRAV(DIRECT)=PAIRAV(DIRECT)+IPAIR
      AVPER(DIRECT)=AVPER(DIRECT)+PERPL(DIRECT)
      WEARAV(DIRECT)=WEARAV(DIRECT)+WEAR(DIRECT)
      STDDEV=STDDEV+WEAR(DIRECT)*WEAR(DIRECT)
      DENOM=DENOM+IPAIR
   25 CONTINUE
 1000 WRITE(OUTFIL,230)PROF,FN(FILE,1),FN(FILE,2),THERA,
     $SKEW,PENET,PAIRS(1),WEAR(1),PERPL(1),PAIRS(2),WEAR(2),
     $PERPL(2)
  230 FORMAT(I2,') ',2A4,F6.3,F6.2,F7.3,2(I6,F8.3,F5.0))
C
C     Now to calculate some averaged wear statistics.
C
      DO 26 DIRECT=1,2
      PAIRAV(DIRECT)=PAIRAV(DIRECT)/NPROF
      AVPER(DIRECT)=AVPER(DIRECT)/NPROF
   26 WEARAV(DIRECT)=WEARAV(DIRECT)/NPROF
      WEARAV(3)=(WEARAV(1)+WEARAV(2))/2.
```

```
      RAAVE=RAAVE/NPROF
      SKEWAV=SKEWAV/NPROF
      PENAVE=PENAVE/NPROF
      NPROF2=2*NPROF
      STDDEV=SQRT((STDDEV-NPROF2*WEARAV(3)*WEARAV(3))/
     $(NPROF2-1))
      STDPER=0.
      AVLUMP=0.
      IF(WEARAV(3).EQ.0.)GOTO 27
      STDPER=STDDEV/WEARAV(3)*100.
      AVLUMP=LMPSUM/DENOM
   27 CONTINUE
C
C      Now for some output.
C
      WRITE(OUTFIL,240)PAIRAV(1),WEARAV(1),AVPER(1),
     $                 PAIRAV(2),WEARAV(2),AVPER(2)
  240 FORMAT(69('_'),//,'  Sub ave.',21X,2(I6,F8.3,F5.0))
      WRITE(OUTFIL,250)RAAVE,SKEWAV,PENAVE,WEARAV(3),STDDEV,
     $AVLUMP,STDPER
  250 FORMAT(/,'  Ave. stats ',F5.3,F6.2,F7.3,21X,
     $'Ave. wear',F8.3/52X,'std. dev. ',F7.3/'  The avera',
     $'ge number of lumps worn=',F6.1,11X,'% of ave.',F8.1)
      STOP
      END
```

```
      SUBROUTINE READ1
C
      INTEGER UNIT,FILTYP
      COMMON/A/UNIT,FILTYP,NP,DX,Y(1500),COMENT(40),DATE(3),
     $LABEL(18)
      COMMON/B/JHEADR,TFACT,HFACT,VFACT,TSPEED,MCODE,CUTOFF
      DATA IDAT/'DATA'/,NUM20/'  20'/,NUM76/'  76'/
C     The next few cards determine whether the file is a
C     CALSPAN (FILTYP=1),  or a VPI generated (FILTYP=2)
C     file.
   10 READ(UNIT,100,END=999)LABEL
  100 FORMAT(18A4)
      IF(NUM20.LE.LABEL(1).AND.LABEL(1).LE.NUM76)GOTO 1
      IF(LABEL(1).EQ.IDAT)GOTO 2
C     If NUM is between 20 and 76 inclusive, it must be the
C     first four characters of a CALSPAN generated file.
C     If LABEL(1) is equal to 'DATA', it must be the first
C     four characters of a VPI generated file.
C     If LABEL(1) is neither, most likely we've hit an
C     information line at the beginning or the end of a file
C     of profile(s).  Let's see what's on the next line...
      GOTO 10
  999 CONTINUE
C     No need to rewind since we're going to abandon this
C     unit number.
      UNIT=UNIT+1
      GOTO 10
    1 BACKSPACE UNIT
      FILTYP=1
      DX=3.33
      READ(UNIT,200)JHEADR,(COMENT(I),I=1,40),NP,TFACT,
     $HFACT,VFACT,TSPEED,(DATE(I),I=1,3),MCODE,CUTOFF
  200 FORMAT(I4,30A4/10A4,I4,4E12.5,3A4,I10,E12.5)
      READ(UNIT,300)(Y(I),I=1,NP)
  300 FORMAT(10(1X,E12.5))
      RETURN
    2 BACKSPACE UNIT
C     Since the data were apparently VPI generated...
      FILTYP=2
      READ(UNIT,400)NP,DX
  400 FORMAT(42X,I4,13X,E12.5)
      READ(UNIT,500)(Y(I),I=1,NP)
  500 FORMAT(8E10.3)
      RETURN
      END
```

```
      SUBROUTINE NORM1(AVE,SLOPE)
C
C     AVE= 1 => No correction for the average is desired.
C        = 2 => A correction for the average is desired.
C   SLOPE= 1 => No correction for slope is desired.
C        = 2 => A correction for slope is desired.
      INTEGER UNIT,AVE,SLOPE,FILTYP
      REAL M
      COMMON/A/UNIT,FILTYP,NP,DX,Y(1500),COMENT(40),DATE(3),
     $LABEL(18)
C     This subroutine fits a best fit straight line through
C     a data set submitted to it, by the method of least
C     squares.  It also alters the profile values to make
C     the average value equal to 0. if requested.
      IF(AVE.NE.1.AND.AVE.NE.2.OR.SLOPE.NE.1.AND.SLOPE.NE.2)
     $STOP
      IF (AVE.EQ.1 .AND. SLOPE.EQ.1) RETURN
      IF (SLOPE .EQ.1) GO TO 3
      SUMY=0.
      SUMXY=0.
      DO 1 I=1,NP
      SUMY=SUMY+Y(I)
    1 SUMXY=SUMXY+I*Y(I)
      M=(12.*SUMXY - 6*(NP+1)*SUMY)/(NP*(NP*NP-1))
      YAVE=SUMY/NP
      YINTER=YAVE-((NP+1)/2.)*M
C     These confirmed series methods for least squares slope
C     and Y intercept can be found in Whitehouse, Tribology,
C     Vol. 7, 1974, p. 249.
      IF(AVE.EQ.1)YINTER=YINTER-YAVE
      DO 2 I=1,NP
    2 Y(I)=Y(I) - M*I - YINTER
C     The above statement deserves an explanation.  YAVE is
C     the average Y value.  If 'AVE'=1, no correction for
C     the average is desired.  Since the least squares fit
C     used here corrects automatically for the average,
C     the average must be added back.  If the correction is
C     desired, 'YAVE' will not be subtracted from 'YINTER',
C     and the automatic correction will not be overriden.
      RETURN
    3 SUMY=0.
      DO 4 I=1,NP
    4 SUMY=SUMY+Y(I)
      YAVE=SUMY/NP
      DO 5 I=1,NP
    5 Y(I)=Y(I)-YAVE
      RETURN
      END
```

```
      SUBROUTINE RANK1 (IDIRE,NP,Y)
C
C     This very efficient ordering routine is based on an
C     algorithm of D. L. Shell (Comm. ACM, July 1959).
C     It orders an array Y of length NP in descending
C     (IDIRE=1) ar ascending (IDIRE=-1) order.
C     (Copied from p.346 of 'Intro. to Stat. with Fortran.')
      DIMENSION Y(1500)
      L=NP
    1 L=L/2
      IF (L) 2,2,3
    2 RETURN
    3 M=NP-L
      DO 6 I=1,M
      J=I
    4 JJ=J+L
      IF (IDIRE.EQ.-1) GO TO 777
C     Going to 777 is for arrays which are to be
C     ranked in ascending order.
      IF (Y(J)-Y(JJ)) 5,6,6
  777 CONTINUE
      IF (Y(J)-Y(JJ)) 6,6,5
    5 Y1=Y(J)
      Y(J)=Y(JJ)
      Y(JJ)=Y1
      J=J-L
      IF (J) 6,6,4
    6 CONTINUE
      GO TO 1
      END
```

Output of program WEAR3 05-01-80

BAR=0.1140, Slider length (mm)=0.5630, Non-normalized
Shear angle (deg)=12.8, Slider width (mm)=0.563,
Elongation ratio, G,= 4.8 .
The combined pin and lay correction=0.5000 .

FILE ID (FN)	STATISTICS Ra (um)	skew	penet (um)	WEAR VOLUME (cu.mm/km) Forward Pairs	Wear	%Full	Backward Pairs	Wear	%Full
1) B32A	0.80	-0.69	1.25	12	14.703	10.	11	22.959	13.
2) B32B	0.92	-0.23	1.30	11	14.710	4.	12	29.978	9.
3) B32C	1.04	-0.30	1.48	10	11.035	3.	6	14.673	28.
4) B32D	0.87	-0.60	0.88	13	19.924	7.	15	21.514	11.
Sub ave.				11	15.093	6.	11	22.281	15.
Ave stats.	0.91	-0.46	1.23				Ave. wear		18.687
							std. dev.		6.113
The average number of lumps worn= 151.3							% of ave.		32.7

10. APPENDIX B: DESCRIPTION AND LISTING OF WEARL

DESCRIPTION AND LISTING OF WEARL

This appendix contains a description and a listing of the subroutine WEARL. This subroutine examines the entire profile for wear sites and calculates the quantities at each site. The philosophy is as follows: Each point Y(K) in the profile is examined in light of the conditions encountered at the past point Y(K-1). The conditions as of the last point are indicated by the value of the integer variable ADDING in the following way:

ADDING =

- 0 The last point wasn't contained in a wear site. Nothing was adding.
- 1 A wear site is in progress. Only the wedge was adding.
- 2 A wear site is in progress. Only the void was adding.
- 3 A wear site is in progress. Both a wedge and a void were adding.

A more detailed explanation of each of these conditions will follow.

Some variable names require explanation. HPOLY is the value of altitude, or height of the bottom surface of the polymer, and is supplied to the WEARL subroutine by the host program. Y(K) is the value of the height of the profile point currently under consideration. Y(K-1) is the value of the profile point immediately to the left of the point currently under consideration. YWEDGE is the height of the modeled wedge at the current point; and YWOLD is the value of the wedge point immediately to the left of the current location.

The remaining text of this appendix contains a graphic development of the ADDING = 1, 2, and 3 sections of WEARL; the first possibility on the ADDING = 1 page is reviewed in detail as an example.

Figure B1 shows the sketch of an element of a wedge to be added to the currently adding wedge area. The five significant points have been labeled. The program is considered to be at the K^{th} position in the profile. ADDING equals 1 since at the $K-1^{th}$ position only the wedge was adding. The incremental wedge area (shaded) will be added to the current wedge area. Since at the K^{th} position the wedge hasn't yet terminated and a void hasn't yet started, the subroutine will exit this section with ADDING still equal to 1 and go on the next point (K+1). All the other cases presented are described by similar means.

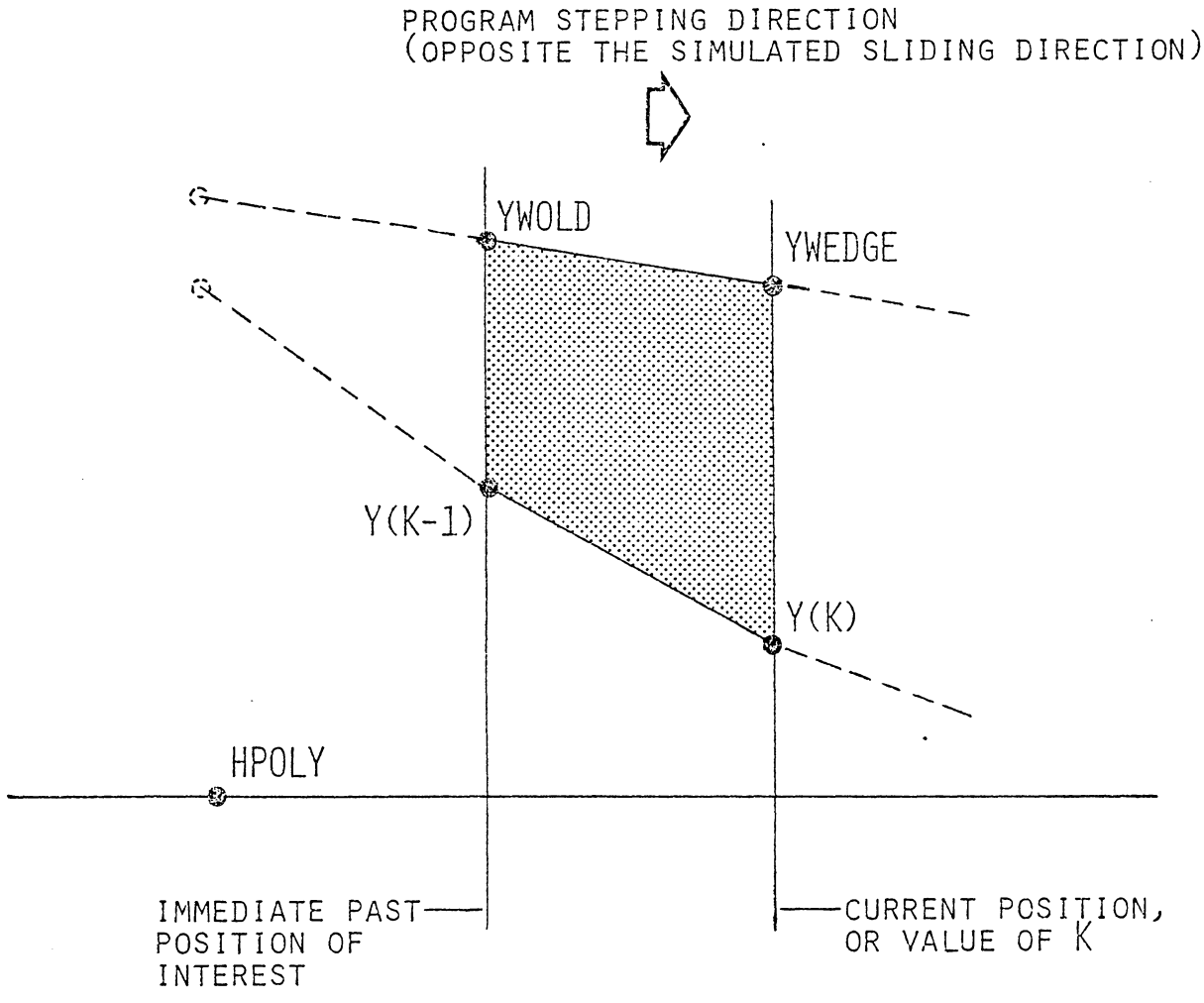

Figure B1. Illustration of first permutation of ADDING = 1 entries.

IF(ADDING.EQ.1)GOTO 100 , Then: IF...

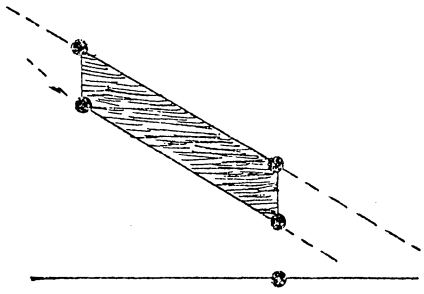

HPOLY ≤ Y(K) ≤ YWEDGE GOTO 110

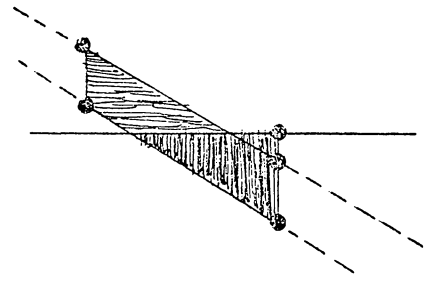

Y(K) ≤ YWEDGE < HPOLY GOTO 140

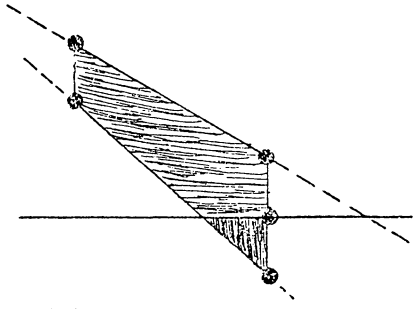

Y(K) < HPOLY < YWEDGE GOTO 120

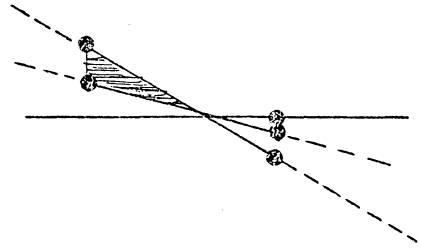

YWEDGE ≤ Y(K) ≤ HPOLY GOTO 150

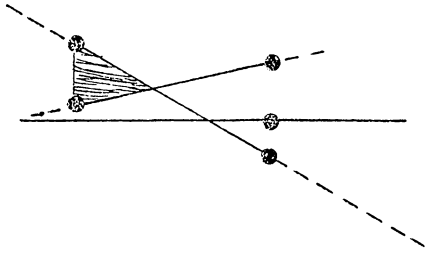

YWEDGE < HPOLY < Y(K) GOTO 130

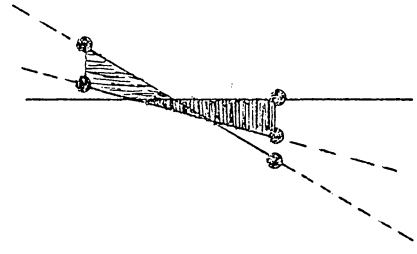

YWEDGE ≤ Y(K) ≤ HPOLY GOTO 150, then GOTO 155

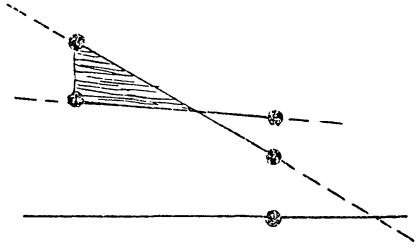

HPOLY ≤ YWEDGE ≤ Y(K) GOTO 130

Figure B2. Permutations of ADDING = 1.

IF(ADDING.EQ.2)GOTO 200 , Then: IF...

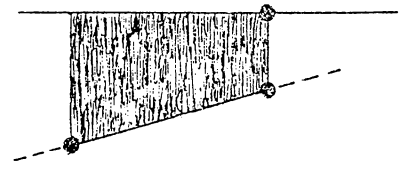

Y(K) < HPOLY GOTO 210

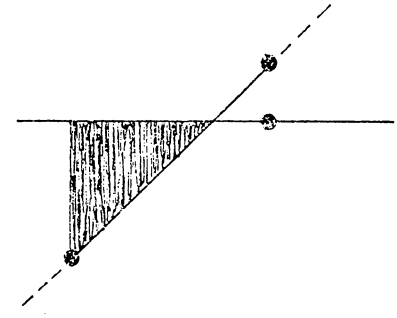

Y(K) ≥ HPOLY GOTO 220

Figure B3. Permutations of ADDING = 2.

IF(ADDING.EQ.3)GOTO 300 , Then: IF...

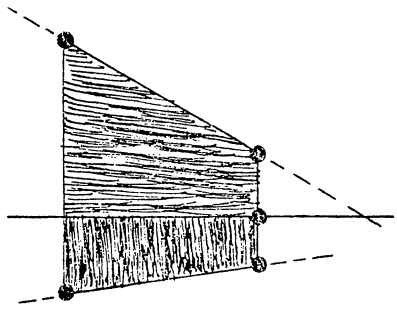

YWEDGE > HPOLY > Y(K) GOTO 310

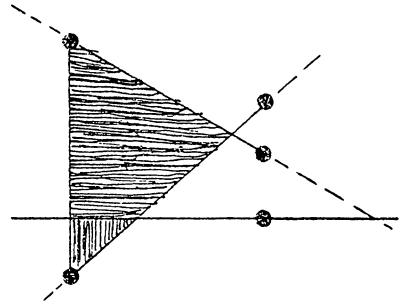

Y(K) ≥ HPOLY and
Y(K) ≥ YWEDGE GOTO 340

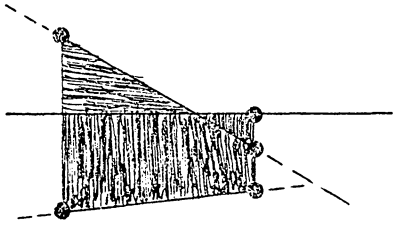

HPOLY > Y(K) and
YWEDGE ≤ HPOLY GOTO 320

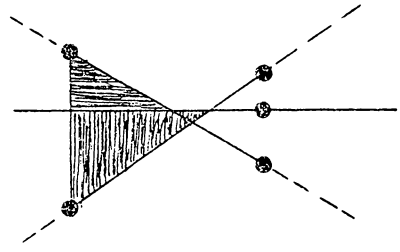

Y(K) ≥ HPOLY and
Y(K) ≥ YWEDGE GOTO 340
then
GOTO 345

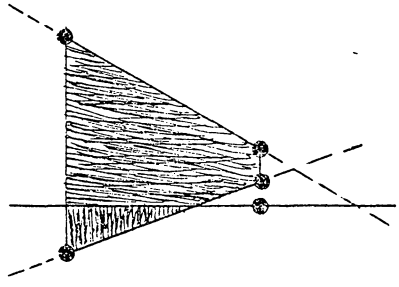

YWEDGE > Y(K) ≥ HPOLY GOTO 330

Figure B4. Permutations of ADDING = 3.

```
C ***************************************************************
C *                                                             *
C *   Polymer Wear Simulation Subroutine WEARL                  *
C *   Written Fall 1979, by John H. Herold                      *
C *                                                             *
C ***************************************************************
C
      SUBROUTINE WEARL(NP,IBEGIN,Y,HPOLY,DX,PAIRS)
      INTEGER TERMIN,ADDING,PAIR,PAIRS
      COMMON/D/TERMIN,WL(200),WA(200),VA(200),ICAP(200),
     $TANANG,LOC(200)
      DIMENSION Y(1500)
      DYCRIT=DX*TANANG
      DYCRI2=DYCRIT/2.
      ADDING=0
      PAIR=0
      IBEGIN=IBEGIN+1
      DO 4 K=IBEGIN,NP
      IF(ADDING.EQ.0)GOTO 2
    1 IF(ADDING.EQ.2)GOTO 200
      YWOLD=YWEDGE
      YWEDGE=YWOLD-DYCRIT
      IF(ADDING.EQ.1)GOTO 100
      IF(ADDING.EQ.3)GOTO 300
C *** If the program get's here, a branching error occurred.
      GOTO 998
    2 CONTINUE
C     This is the searching section, and the program loops
C     through here watching for a wedge to start.
      IF(Y(K-1).LE.HPOLY)GOTO 3
      YFALL=Y(K-1)-Y(K)
      IF(YFALL.LE.DYCRIT)GOTO 3
C     Bingo! We've got a wedge starting!
      PAIR=PAIR+1
      LOC(PAIR)=K
      IF(PAIR.GT.200)GOTO 999
      YWEDGE=Y(K-1)
      WA(PAIR)=0.
      WL(PAIR)=0.
      VA(PAIR)=0.
```

```
      ADDING=1
      GOTO 1
  100 CONTINUE
C     Given that ADDING=1, what can happen next?
      IF(YWEDGE.GE.Y(K).AND.Y(K).GE.HPOLY)GOTO 110
      IF(YWEDGE.GT.HPOLY.AND.HPOLY.GT.Y(K))GOTO 120
C     OK, the wedge terminates, but in which of five ways?
      IF(Y(K).GT.YWEDGE.AND.Y(K).GE.HPOLY)GOTO 130
      IF(HPOLY.GT.YWEDGE.AND.YWEDGE.GE.Y(K))GOTO 140
      IF(HPOLY.GE.Y(K).AND.Y(K).GE.YWEDGE)GOTO 150
C *** If the program get's here, a branching error occurred.
      GOTO 998
  110 CONTINUE
C     Continuing wedge, no void.
      WL(PAIR)=WL(PAIR)+DX
      WA(PAIR)=WA(PAIR)+DX*(YWOLD-DYCRI2-(Y(K-1)+Y(K))/2.)
      GOTO 3
  120 CONTINUE
C     Continuing wedge, void starting to add.
      WL(PAIR)=WL(PAIR)+DX
      FRCBEL=(HPOLY-Y(K))/(Y(K-1)-Y(K))
      VADD=0.5*(FRCBEL*DX)*(HPOLY-Y(K))
      VA(PAIR)=VA(PAIR)+VADD
      WA(PAIR)=WA(PAIR)+DX*(YWOLD-DYCRI2-(Y(K-1)+Y(K))/2.)
     $-VADD
      ADDING=3
      GOTO 3
  130 CONTINUE
C     Wedge terminates, void not adding.
      DXW=DX*(YWOLD-Y(K-1))/(Y(K)-Y(K-1)+DYCRIT)
      WL(PAIR)=WL(PAIR)+DXW
      WA(PAIR)=WA(PAIR)+0.5*DXW*(YWOLD-Y(K-1))
      ADDING=0
      GOTO 3
  140 CONTINUE
C     Wedge terminates, but void starts adding soon enough.
      FRCBEL=(HPOLY-Y(K))/(Y(K-1)-Y(K))
      VADD=0.5*(FRCBEL*DX)*(HPOLY-Y(K))
      VA(PAIR)=VA(PAIR)+VADD
      VSUBTR=0.5*(HPOLY-YWEDGE)**2/TANANG
      WA(PAIR)=WA(PAIR)+DX*(YWOLD-DYCRI2-(Y(K-1)+Y(K))/2.)
     $-(VADD-VSUBTR)
      DXW=(YWOLD-HPOLY)/TANANG
      WL(PAIR)=WL(PAIR)+DXW
      ADDING=2
      GOTO 3
  150 CONTINUE
C     The wedge terminates, but the void may or may not
C     communicate.
```

```
      DXW=DX*(YWOLD-Y(K-1))/(Y(K)-Y(K-1)+DYCRIT)
      DXV=DX*(Y(K-1)-HPOLY)/(Y(K-1)-Y(K))
      WA(PAIR)=WA(PAIR)+0.5*(YWOLD-Y(K-1))*DXW
      IF(DXW.GT.DXV)GOTO 155
C     No communication, just add end of wedge (already done)
C     and quit.
      WL(PAIR)=WL(PAIR)+DXW
      ADDING=0
      GOTO 3
  155 CONTINUE
C     Ah, we have communication by a finite border!
      DXWV=(YWOLD-HPOLY)/TANANG
      WL(PAIR)=WL(PAIR)+DXWV
      VSUBTR=0.5*(DXWV-DXV)*((DXW-DXWV)*TANANG)
      WA(PAIR)=WA(PAIR)-VSUBTR
      VA(PAIR)=VA(PAIR)+0.5*(DX-DXV)*(HPOLY-Y(K))
      ADDING=2
      GOTO 3
  200 CONTINUE
C     The void only is adding.
      IF(Y(K).LT.HPOLY)GOTO 210
      IF(Y(K).GE.HPOLY)GOTO 220
C *** If the program get's here, a branching error occurred.
      GOTO 998
  210 CONTINUE
C     No problem, void continues.
      VA(PAIR)=VA(PAIR)+DX*(HPOLY-(Y(K)+Y(K-1))/2.)
      GOTO 3
  220 CONTINUE
C     The void terminates.  We'll add it in and then quit.
      DXV=DX*(HPOLY-Y(K-1))/(Y(K)-Y(K-1))
      VA(PAIR)=VA(PAIR)+0.5*(HPOLY-Y(K-1))*DXV
      ADDING=0
      GOTO 3
  300 CONTINUE
C     Void and wedge are both adding.
      IF(HPOLY.GT.Y(K).AND.YWEDGE.GT.HPOLY)GOTO 310
      IF(HPOLY.GT.Y(K).AND.YWEDGE.LE.HPOLY)GOTO 320
      IF(HPOLY.LE.Y(K).AND.YWEDGE.GT.Y(K))GOTO 330
      IF(Y(K).GE.HPOLY.AND.Y(K).GE.YWEDGE)GOTO 340
C *** If the program get's here, a branching error occurred.
      GOTO 998
  310 CONTINUE
C     Wedge and void continue adding nicely.
      WL(PAIR)=WL(PAIR)+DX
      WA(PAIR)=WA(PAIR)+DX*(YWOLD-DYCRI2-HPOLY)
      VA(PAIR)=VA(PAIR)+DX*(HPOLY-(Y(K-1)+Y(K))/2.)
      GOTO 3
  320 CONTINUE
```

```
C       Wedge terminates, void continues adding.
        DXW=(YWOLD-HPOLY)/TANANG
        WL(PAIR)=WL(PAIR)+DXW
        WA(PAIR)=WA(PAIR)+0.5*DXW*(YWOLD-HPOLY)
        VA(PAIR)=VA(PAIR)+DX*(HPOLY-(Y(K-1)+Y(K))/2.)
        ADDING=2
        GOTO 3
  330 CONTINUE
C       The wedge continues but the void stops
C       (at least for now).
        WL(PAIR)=WL(PAIR)+DX
        DXV=DX*(HPOLY-Y(K-1))/(Y(K)-Y(K-1))
        VADD=0.5*DXV*(HPOLY-Y(K-1))
        VA(PAIR)=VA(PAIR)+VADD
        WA(PAIR)=WA(PAIR)+DX*(YWOLD-DYCRI2-(Y(K)+Y(K-1))/2.)
       $-VADD
        ADDING=1
        GOTO 3
  340 CONTINUE
C       Both the void and the wedge terminate here, but how?
        DXV=DX*(HPOLY-Y(K-1))/(Y(K)-Y(K-1))
        VADD=0.5*DXV*(HPOLY-Y(K-1))
        VA(PAIR)=VA(PAIR)+VADD
        DXW=DX*(YWOLD-Y(K-1))/(Y(K)-Y(K-1)+DYCRIT)
        IF(DXW.LT.DXV)GOTO 345
C       Wedge terminates with, or after void.
        WA(PAIR)=WA(PAIR)+0.5*DXW*(YWOLD-Y(K-1))-VADD
        WL(PAIR)=WL(PAIR)+DXW
        ADDING=0
        GOTO 3
  345 CONTINUE
C       The wedge terminates before the void does.
        DXWNEW=(YWOLD-HPOLY)/TANANG
        WA(PAIR)=WA(PAIR)+0.5*DXWNEW*(YWOLD-HPOLY)
        WL(PAIR)=WL(PAIR)+DXWNEW
        ADDING=0
        GOTO 3
    3 CONTINUE
C       WRITE(TERMIN,233)K,PAIR,WA(PAIR),WL(PAIR),VA(PAIR)
C 233 FORMAT(I3,2X,I1,3(2X,F10.5))
    4 CONTINUE
        PAIRS=PAIR
        IF(PAIRS.EQ.0)RETURN
C       Let's now determine the integral capacities
C       of each pair.
        DO 5 PAIR=1,PAIRS
        CAP=VA(PAIR)/WA(PAIR)
        ICAP(PAIR)=CAP+1
    5 CONTINUE
```

```
      RETURN
  998 WRITE(TERMIN,1000)
 1000 FORMAT(/,'******  An error has occurred in branching,'
     $,/,'causing the program to terminate. ********')
      STOP
  999 WRITE(TERMIN,1010)
 1010 FORMAT('********** The number of pairs exceeded 200,'
     $,/,'causing the program to terminate within ',
     $'subroutine WEARL *****')
      STOP
      END
```

The vita has been removed from the scanned document

A MODEL FOR ABRASIVE POLYMER WEAR

by

John Henry Herold II

(ABSTRACT)

The abrasive mechanism of polymer wear is dominant in the startup, or "breakin", stage of polymer/steel sliding systems. This mechanism controls the polymer wear rate until the voids in the hard metal surface are filled, much like the filling observed with a file when used on soft metals. This regime of polymer wear is modeled on an event-by-event basis. The model utilizes a digitized profile of the metal surface, bulk polymer properties such as flow pressure and elongation at break, and a few system parameters such as load and slider geometry. The predictions of the model are compared with experimental data. The predicted wear rates are within a factor of 3 of the measured wear rates for polymers with glass transition temperatures, T_g, above the interfacial temperature (rigid PVC and PCTFE). The validity of the model is shown to be related to the ductile or brittle behavior of the sliding polymer.